European Journal of Medicinal Chemistry 212 (2021) 113124

Contents lists available at ScienceDirect

European Journal of Medicinal Chemistry

journal homepage: http://www.elsevier.com/locate/ejmech

Research paper

Design, synthesis and biological evaluation of new benzoxazolone/benzothiazolone derivatives as multi-target agents against Alzheimer's disease

Merve Erdogan [a], Burcu Kilic [a], Rahsan Ilıkcı Sagkan [b], Fatma Aksakal [c], Tugba Ercetin [d], Hayrettin O. Gulcan [d], Deniz S. Dogruer [a, *]

[a] Department of Pharmaceutical Chemistry, Faculty of Pharmacy, Gazi University, Ankara, Turkey
[b] Department of Medical Biology, Faculty of Medicine, Uşak University, Uşak, Turkey
[c] Department of Chemistry, Hacettepe University, Ankara, Turkey
[d] Department of Pharmaceutical Chemistry, Faculty of Pharmacy, Eastern Mediterranean University, Gazimagosa, Cyprus

ARTICLE INFO

Article history:
Received 14 October 2020
Received in revised form
27 November 2020
Accepted 18 December 2020
Available online 24 December 2020

Keywords:
Alzheimer's disease
Benzoxazolone
Benzothiazolone
Cholinesterase inhibitory activity
Anti-inflammatory
Molecular docking

ABSTRACT

In this study, four series of compounds with benzoxazolone and benzothiazolone cores were designed, synthesized and evaluated as multifunctional agents against Alzheimer's disease (AD). Additionally, in order to shed light on the effect of the carbonyl groups of benzoxazolone/benzothiazolone, benzoxazole/benzothiazole-containing analogues were also synthesized and evaluated. Inhibition potency of all final compounds towards cholinesterase enzymes and their antioxidant activity were tested. Subsequently, the anti-inflammatory activity, cytotoxicity, apoptosis, and Aβ aggregation inhibition tests were also performed for selected compounds. The results indicated that compounds **11c**, a pentanamide derivative with benzothiazolone core, and **14b**, a keton derivative with benzothiazolone core, were considered as promising multi-functional agents for further investigation against AD. The reversibility, kinetic and molecular docking studies were also performed for the compounds with the highest AChE **14b** (*ee*AChE IC_{50} = 0.34 μM, *hu*AChE IC_{50} = 0.46 μM) and BChE **11c** (*eq*BChE IC_{50} = 2.98 μM, *hu*BChE IC_{50} = 2.56 μM) inhibitory activities.

© 2020 Elsevier Masson SAS. All rights reserved.

1. Introduction

Alzheimer's disease (AD), accounting for about 70% of all dementia cases, is a progressive neurodegenerative brain disease in elderly people. The 2019 report of Alzheimer Disease International has been estimated that there are more than 50 million people living with dementia worldwide and the incidence of the disease will triple by 2050 because of the increase in the average life expectancy. Accordingly, AD poses a great problem for global health [1,2].

Despite many scientific efforts, the mechanism underlying the pathogenesis of AD is not exactly explained due to its complex and multifactorial characteristics. However, many factors involved in the development of AD (e.g., amyloid-β (Aβ) plaques and hyperphosphorylated neurofibrillary tangle (NFT) formations, acetylcholine (ACh) deficiency, neuroinflammation, oxidative stress, and excitotoxicity) have been well determined [3,4]. The neurotransmitter ACh deficiency in specific regions of the brain associated with cognitive functions results in progressive memory and orientation loss and other cognitive impairments combined with behavioral and neuropsychiatric disturbances. Thus, drugs including donepezil, rivastigmine, and galantamine, which can increase ACh levels through the inhibition of cholinesterase enzymes have been developed [5,6]. However, these drugs can only slow down the progression of cognitive function impairments. Therefore, the research studies focus on the development of compounds that may be effective on different pathologies of the disease along with cholinesterase inhibitory activity [7].

Recently, many studies have revealed that neuroinflammation plays a fundamental role in AD. It has been reported that an incessant immune response in the brain is not only associated with neurodegeneration but it also facilitates and exacerbates both Aβ and NFT pathologies [8]. Furthermore, it has been suggested that chronic neuroinflammation may be a central mechanism driving Aβ

* Corresponding author.
E-mail addresses: dogruer@gazi.edu.tr, denizdogruer2002@yahoo.com (D.S. Dogruer).

https://doi.org/10.1016/j.ejmech.2020.113124
0223-5234/© 2020 Elsevier Masson SAS. All rights reserved.

pathology and progression. In AD, a disruption in the balance of anti-inflammatory and pro-inflammatory signals results in chronic neuroinflammation, which is attributed to the activation of microglia cells and the release of numerous cytokines [8,9]. Microglia, the resident immune cells within the central nervous system (CNS), are activated once they recognize a threat to the CNS. Several investigations have demonstrated that activated microglia phagocytose Aβ, but after prolonged activation of periods, they are no longer able to phagocytose Aβ. Nevertheless, it has been indicated that their capacity to produce pro-inflammatory cytokines is unaffected. This situation makes overall clearance of Aβ become dangerous [10]. Moreover, the continued release of pro-inflammatory cytokines from microglia worsens the neuroinflammation and contribute to neurodegeneration. Recent studies have demonstrated that reducing the levels of inflammatory markers such as interleukin-1β (IL-1β), interleukin-6 (IL-6), tumor necrosis factor-α (TNF-α) and nitric oxide (NO) released from stimulated microglia and other immune cells may be effective for the treatment of AD [11–13].

Oxidative stress (OS) or nitrative stress (NS) is a condition caused by increased reactive oxygen species (ROS) and reactive nitrogen species (RNS) concentrations in cells when the antioxidant defense system is overwhelmed. The concentrations of ROS and RNS, steadily produced and eliminated during cellular reactions, are the key factor of their effect. At very low concentrations, they are known to play vital role in many biological processes such as cell growth, cell signaling, smooth muscle relaxation, immune responses. However, OS/NS, resulting from the increased cellular concentration of ROS/RNS, leads to the oxidation of cellular macromolecules such as lipids, proteins, and DNA, which is involved in the development of many pathophysiological conditions. Accordingly, there are several experimental data supporting the idea that OS is associated with both the initiation and progression of AD. Thus, compounds with antioxidant activity might be useful for the treatment of AD [14–16].

Benzoxazolone and benzothiazolone rings which are bioisosteres of each other have attracted attention because of their capacity to mimic a phenol or catechol [17]. In addition, these cores have been used as privileged scaffolds in the design of new compounds due to their wide range of biological properties as well as anti-inflammatory [18–21] and antioxidant [22] activities. Moreover, various tertiary amine moieties reported as cholinesterase inhibitory pharmacophores were used to derivatization of the synthesized compounds in the present study [23,24].

Since a drug with a single-target mechanism of action cannot be effective in the treatment of complex and multifactorial diseases such as Alzheimer's disease, the development of multi-target compounds that can interact with two or more targets associated with AD pathogenesis has been adopted as a more effective treatment strategy [7,25,26].

In the light of these facts and as a continuation of our research for new anti-Alzheimer compounds [27–30], we designed and synthesized new propanamide derivatives in which the side chain at the 6th positions of the 3-methyl-benzoxazolone and 3-methyl-benzothiazolone rings terminate with tertiary amine structures. After the cholinesterase inhibitory activities of the synthesized compounds were examined, the compounds with the highest AChE (acetylcholinesterase) and BChE (butyrylcholinesterase) inhibitory activities were determined. Subsequently, with the hope of improving AChE/BChE inhibitory activity, new compounds were designed by the structural modifications of the compounds. For this purpose, firstly butanamide and pentanamide derivatives were prepared to find the optimal length of the linker. Secondly, the ketone derivatives were synthesized to evaluate the effect of the functional group. Finally, to get a better insight into the effect of the ring system, 2-phenylbenzoxazole/benzothiazole derivative-two compounds were synthesized by replacing the carbonyl group at the benzoxazolone/benzothiazolone rings with the phenyl ring. As a result, a total of 39 new final compounds were synthesized, including the propanamide derivative 28 and the 11 compounds obtained by structural modifications of the compounds with the highest AChE (**8g**, **9g**) and BChE inhibitory (**9l**) activities (Fig. 1). Subsequently, inhibition potency of all final compounds towards cholinesterase enzymes and their antioxidant activity were tested. Additionally, the anti-inflammatory activity, cytotoxicity, apoptosis, and Aβ aggregation inhibition tests were also performed for selected compounds. The reversibility, kinetic and molecular docking studies were also performed for the compounds with the highest AChE and BChE inhibitory activity.

2. Result and discussion

2.1. Chemistry

The synthetic routes of intermediates **5**, **6** and final compounds **8a-n**, **9a-n**, **10a-c**, **11a-c**, **14a-c**, **21a-b** are presented in Schemes 1–6, respectively. Compounds **5** and **6** used as the cardinal intermediates in the synthesis of final compounds **8a-n**, **9a-n**, **10a-c**, and **11a-c** were synthesized by the methylation of commercially available 1,3-benzoxazol-2(3*H*)one or 1,3-benzothiazol-2(3*H*)-one rings with dimethyl sulfate followed by nitration with nitric acid and then reduction with $SnCl_2$ [31,32]. In order to synthesize propanamide derivatives bearing benzoxazolone ring, the intermediate **5** was first acylated with 3-chloropropionyl chloride to obtain the intermediate **7**. Then, this compound was reacted with appropriate secondary amines to get the title compounds **(8a-n)**. However, the propanamide derivatives carrying the benzothiazolone ring (**9a-n**) could not be synthesized by the above method, because of low yield. These compounds were prepared by the reaction of intermediate 6 with CAS registered 3-substitutedpropanoic acid derivatives prepared by Michael addition according to our in-house method [30]. To obtain compounds **10a-c** and **11a-c** in the butanamide and pentanamide series respectively were used the following steps. First, the reaction of ethyl 4-bromobutyrate or ethyl 5-bromovalerate with appropriate amines gave corresponding ester derivatives which were further hydrolyzed in %5 NaOH solution to give 4-substitutedbutanoic acid or 5-substitutedpentanoic acid, respectively. Then, compounds **10a-c** and **11a-c** were prepared by the reaction of intermediate **5** or **6** with 4-substitutedbutanoic acid or 5-substitutedpentanoic acid in the presence of EDC and DMAP, as shown in Scheme 4. For preparing compounds **14a-c**, Intermediates **12** and **13** were synthesized by the Friedel-Crafts acylation reaction of 1,3-benzoxazol-2(3H)-one/1,3-benzothiazol-2(3H)-one with 3-chloropropionyl chloride [33]. Then, compounds **14a-c** were obtained by treatment of intermediate **12**, **13** with sodium iodide, potassium carbonate, and suitable amine derivatives. In the synthesis of final compounds **21a-b**, commercially available 2-amino-5-nitrophenol and 2-amino-5-nitrobenzenethiol (**16**) synthesized in our laboratory were used as starting materials. The nitration of 1,3-benzothiazole with nitric acid afforded intermediate **15** [34] that was subsequently hydrolyzed to **16** *(CAS 23451-98-1)* with a 20% solution of potassium hydroxide. Intermediates **17** and **18** were obtained from the reaction of both starting materials with benzoic acid in PPA [35], which were further reduced with iron to provide intermediates **19** and **20** [35]. Then, the reaction of **19** and **20** with 3-(4-benzylpiperazin-1-yl)propanoic acid in the presence of EDC and DMAP gave **21a** and **21b**, respectively.

The chemical structures of recently synthesized compounds were approved by ^{1}H NMR, ^{13}C NMR, HRMS, and elemental analysis.

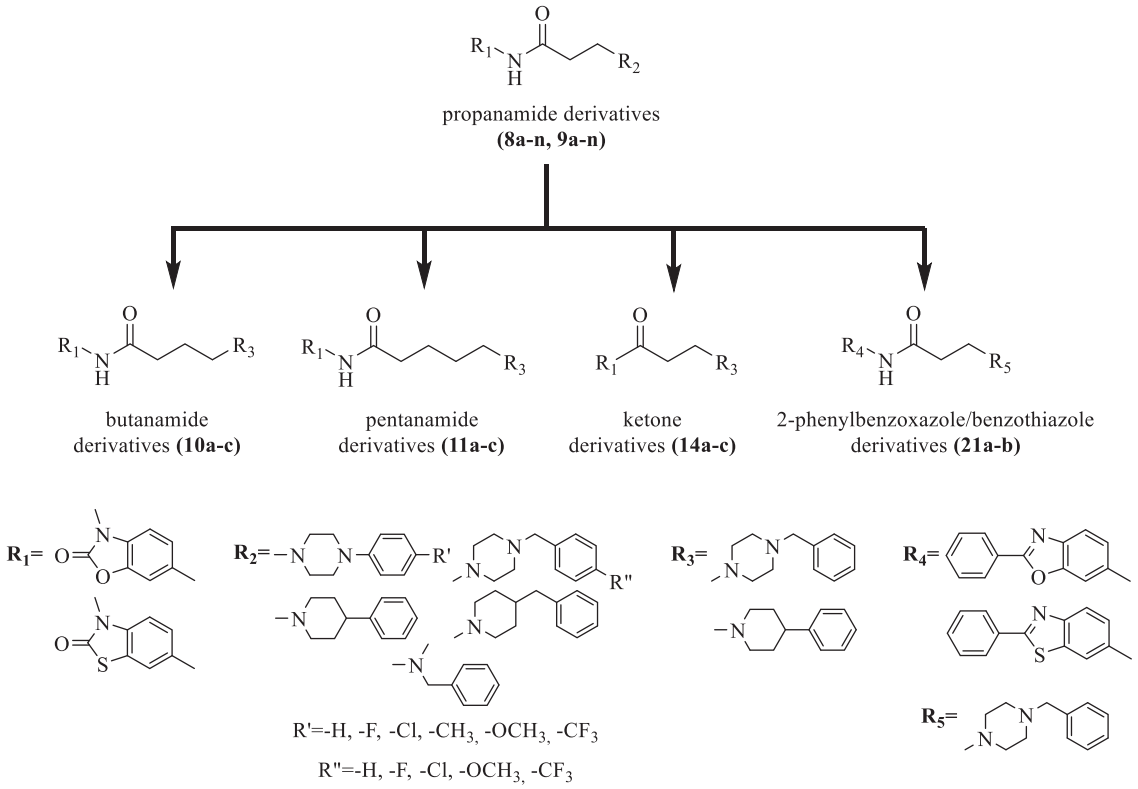

Fig. 1. The general structure of synthesized compounds.

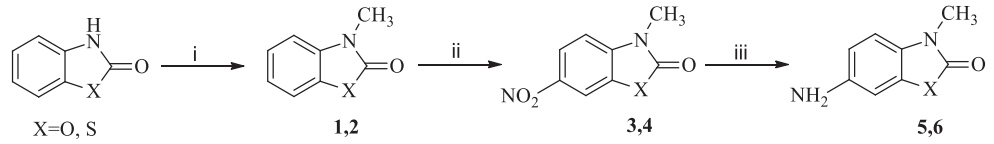

Scheme 1. Synthesis of the compounds **5**–**6**. Conditions and reagents: **(i)** Dimethyl sulfate, 1 M NaOH, 30 min, rt. **(ii)** %65 HNO_3, 1 h, 40 °C. **(iii)** $SnCl_2$, 6 M HCl, EtOH, 30 min, reflux.

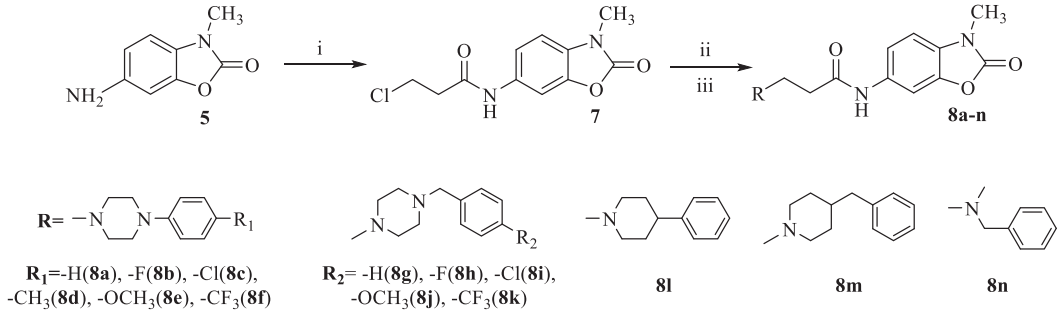

Scheme 2. Synthesis of the compounds **8a-n**. Conditions and reagents: **(i)** 3-Chloropropionyl chloride, DMAP, TEA, DMF, 1 h, rt. **(ii)** NaI, ACN, reflux, 2 h. **(iii)** Amine derivative, K_2CO_3, 3 h, rt.

2.2. Cholinesterase inhibitory activities

Initially, the percent inhibition of final compounds on AChE (from electric eel) and BChE (from equine serum) were evaluated by the modified Ellman's method using donepezil (10 μM) as the reference compound. Subsequently, IC_{50} values of final compounds showing inhibition above 50% were calculated and the results are reported in Table 1.

Concerning AChE inhibition of propanamide derivatives (**8a-n**; **9a-n**), nonsubstituted benzylpiperazine-bearing compounds **8g** and **9g** were more active than other compounds. Between the two compounds, the stronger inhibitor was compound **9g** with benzothiazolone core (IC_{50} = 2.34 μM) followed by compound **8g** with benzoxazolone core (IC_{50} = 6.94 μM). When the effect of the substituents at the para position of the phenyl ring of benzylpiperazine on the activity was evaluated, it was observed that fluorine at the

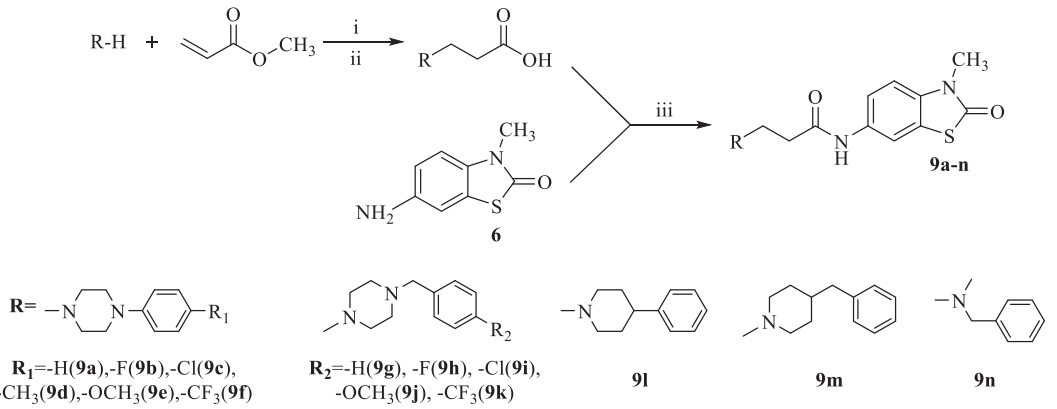

Scheme 3. Synthesis of the compounds **9a-n**. Conditions and reagents: **(i)** DCM, overnight, rt. **(ii)** %5 NaOH, 2 h, 40 °C. **(iii)** EDC, DMAP, DCM, overnight, rt.

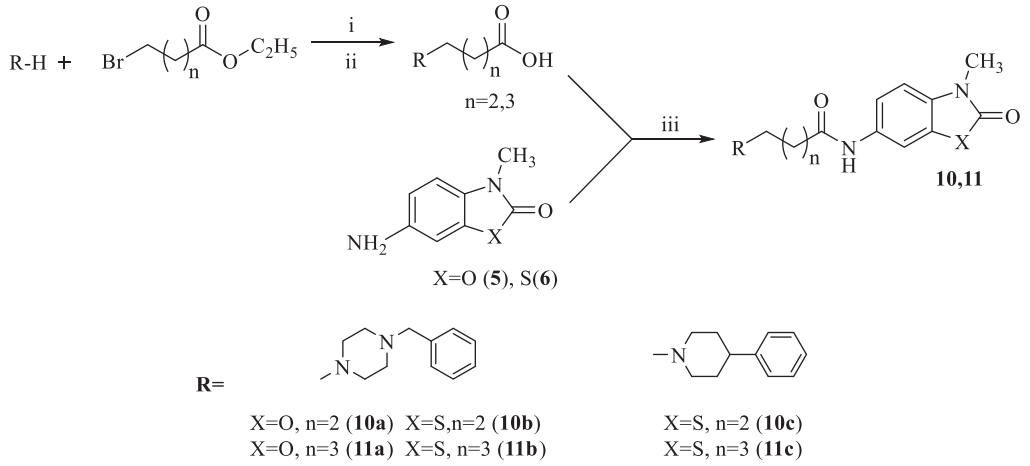

Scheme 4. Synthesis of the compounds **10a-c** and **11a-c**. Conditions and reagents: **(i)** ACN, K_2CO_3, 6 h, reflux**. (ii)** %5 NaOH, 2 h, 40 °C. **(iii)** EDC, DMAP, DCM, overnight, rt.

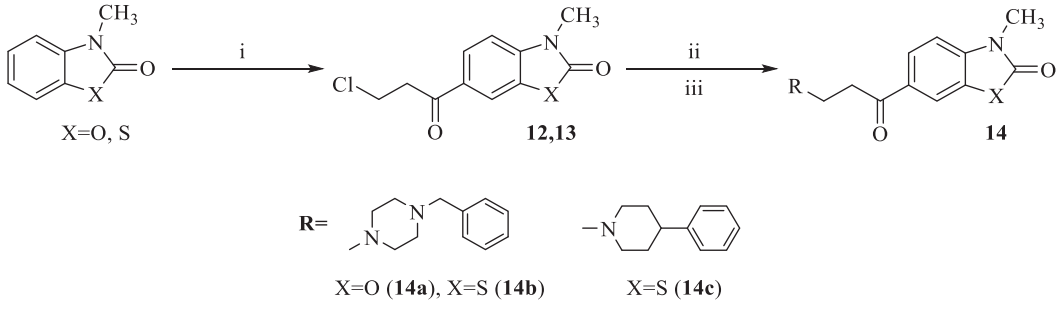

Scheme 5. Synthesis of the compounds **14a-c**. Conditions and reagents: **(i)** 3-Chloropropionyl chloride, $AlCl_3$, DMF, 2 h, 45 °C. **(ii)** NaI, ACN, reflux, 2 h. **(iii)** Amine derivative, K_2CO_3, 3 h, rt.

para position (**8h** IC_{50} = 16.10 μM and **9h** IC_{50} = 7.09 μM) reduced inhibitor activity approximately 2.5 times, while the other substituents abolished the activity compared to their nonsubstituted benzylpiperazine counterpart. The results showed that substitutions on the para position of the phenyl ring were not tolerated except for fluorine substituent. Similarly, as with nonsubstituted benzylpiperazine derivatives, 4-fluorobenzylpiperazine-carrying compound **9h** with benzothiazolone core was more effective than the corresponding benzoxazolone derivative (compound **8h**). However, the presence of phenylpiperidine, benzylpiperidine, *N*-methylbenzylamine groups, phenylpiperazine, and its derivatives at the side chain significantly decreased or abolished AChE inhibition of the compounds.

As for the BChE inhibition, most of the compounds displayed negligible BChE inhibitory activity except for **9h, 9l, 9m,** and **9n.** Among the active compounds, 4-phenypiperidine-bearing compound **9l** with benzothiazolone core displayed the highest inhibition potential with an IC_{50} value of 11.14 μM. In addition, none of the compounds possessing inhibitory activity on BChE are not benzoxazolone analogues.

Overall, these results showed that benzothiazolone ring is not only important for AChE inhibition but is also critical for BChE

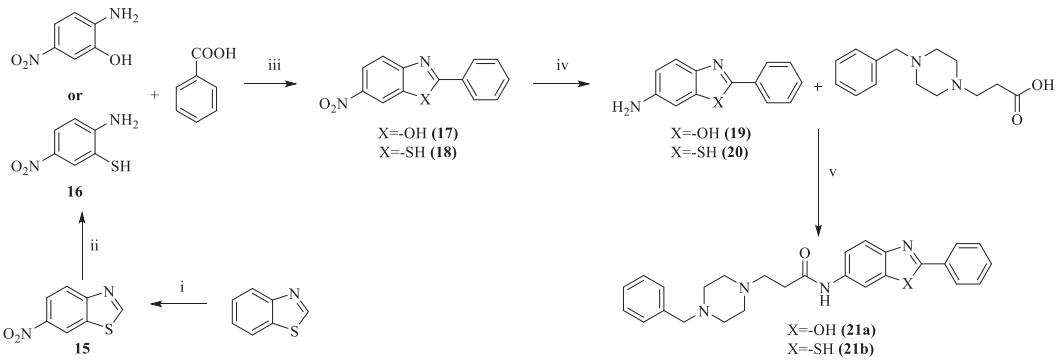

Scheme 6. Synthesis of the compounds **21a-b.** Conditions and reagents: **(i)** H_2SO_4, HNO_3, 45 min, 4–6 °C. **(ii)** %20 KOH, 5 h, reflux **(iii)** PPA, 2 h, 140 °C. **(iv)** Fe, 1.2 N HCl, EtOH, 2 h, reflux. **(v)** EDC, DMAP, DCM, overnight, rt.

inhibition. Furthermore, the benzylpiperazine and 4-phenylpiperidine structures in the propanamide series were determined to be favorable in terms of AChE and BChE inhibition, respectively. In this connection, compound **9g** with the highest AChE inhibition ($IC_{50} = 2.34$ μM) and compound **9l** with the highest BChE inhibition ($IC_{50} = 11.14$ μM) were selected as the hit compounds in the propanamide series. In addition, some final compounds with benzoxazolone core were also synthesized in order to make a comparison in terms of AChE inhibition in new series.

From this point of view, butanamide **(10a-c)** and pentanamide series **(11a-c)** were prepared to examine the effect of the carbon number in the side chain on inhibitory activity. In the butanamide series, compounds **10a** ($IC_{50} = 6.00$ μM) and **10b** ($IC_{50} = 1.96$ μM) were found to slightly increase AChE inhibition compared to compounds in the propanamide series. However, compounds in the pentanamide series reduced AChE inhibition. Regarding BChE inhibition of compounds in butanamide and pentanamide series, Compound **10c** from the butanamide series ($IC_{50} = 9.65$ μM) was more active compared to the propanamide series compound **9l** ($IC_{50} = 11.14$ μM). In addition, compound **11c** ($IC_{50} = 2.98$ μM) in the pentanamide series exhibited the most potent inhibition for BChE among all series, indicating that increasing the side chain length positively affected activity.

In the case of ketone derivatives **(14a-c)**, compound **14b** with the benzothiazolone core possessed the highest AChE inhibitory activity with an IC_{50} value of 0.34 μM among all series, indicating that the ketone function was more suitable for AChE inhibitory activity instead of the amide function.

Regarding compounds **21a** and **21b**, removal of carbonyl group at the second position of benzoxazolone and benzothiazolone rings abolished the cholinesterase inhibition.

Finally, the IC_{50} values of compound **14b** with the highest inhibitory activity against *electric eel* AChE (*ee*AChE) and compound **11c** with the highest inhibitory activity against *equine* BChE (*eq*BChE) were also examined against *human* AChE (*hu*AChE) and *human* BChE (*hu*BChE), respectively. New results were parallel with the results obtained from eeAChE and eqBChE (**14b** *ee*AChE $IC_{50} = 0.34$ μM, *hu*AChE $IC_{50} = 0.46$ μM and **11c** eqBChE $IC_{50} = 2.98$ μM, *hu*BChE $IC_{50} = 2.56$ μM).

2.3. Reversibility studies of 11c and 14b for AChE/BuChE inhibition

A previously described dilution method was employed to test the reversibility of enzyme inhibition observed for the most active compounds in the series (i.e., **14b** for *hu*AChE, and **11c** for *hu*BChE) [36]. Briefly, ten times and a hundred times of IC_{50} concentrations of the inhibitors were incubated with enzyme at 37 °C for 30 min. After this incubation period, the reaction was subsequently diluted 100-fold with substrate solution to give final concentrations of inhibitors 0.1 × IC_{50} and 1 × IC_{50}, respectively. In control studies, inhibitors were replaced with standard inhibitors and buffer. The reaction was further incubated at 37 °C for a further 15 min and the residual enzyme activities were measured, and the results are displayed in bar graphic in Fig. 2 and Table 2 as well. All measurements were carried out in triplicate and are expressed as mean ± SEM.

For reversible enzyme inhibition, the enzyme activities are expected to be recovered to the levels of approximately 90% and 50%, respectively, after 100-fold dilution of the preincubations containing inhibitor concentrations of 10xIC_{50} and 100xIC_{50} [37]. Thus, the results obtained pointed out the reversible inhibitor character of the title molecules under the experimental conditions employed.

2.4. Kinetic studies of enzyme inhibition

To determine the enzyme inhibition types and inhibition constant (K_i) of the two most active molecules, enzyme kinetics studies were carried out on compound **11c** (for *eq*BChE) and **14b** (for *ee*AChE). Lineweaver-Burk plots and replots of the slope versus concentration were utilized to obtain the inhibition constants (K_i), as shown in Fig. 3. Accordingly, compound **11c** was shown to have mixed-type inhibition and compound **14b** was shown to have noncompetitive type inhibition. The obtained K_i values were consistent with the measured IC_{50} values.

2.5. In vitro antioxidant activity

The antioxidant activities of synthesized compounds were tested by the ORAC-FL method (Oxygen Radicals Absorbance Capacity by Fluorescence). The vitamin E analogue Trolox was used as a standard. According to the data in Table 1, all the compounds exhibited good ORAC-FL values within the range of 2.61–4.55 Trolox equivalents at 10 μM concentration. The results indicated that functional group, or atom differences among the synthesized molecules resulted in little or negligible effect on the antioxidant effects determined under the ORAC assay conditions.

2.6. Inhibitory effects of selected compounds on IL-1β, IL-6, TNF-α and NO production

Neuroinflammation plays a vital role in AD and other neurodegenerative diseases. So, preventing the production of inflammatory factors released from activated microglia has been considered to be a promising strategy for the treatment of disease.

Table 1
Cholinesterase inhibitory activities and ORAC results of the synthesized compounds.

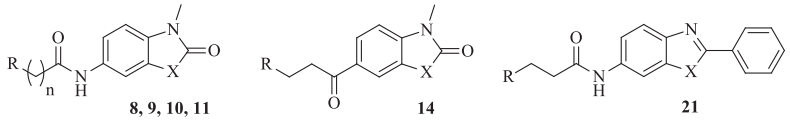

8, 9, 10, 11 **14** **21**

Compd	X	n	R	*ee*AChE		*eq*BChE		ORAC
				% inhibition ± SD (100 μM)	IC_{50} ± SD (μM)	% inhibition ± SD (100 μM)	IC_{50} ± SD (μM)	
8a	O	2	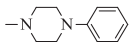	32 ± 3.7	n.t	<%10	n.t	4.02 ± 0.008
8b	O	2	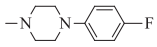	35 ± 3.3	n.t	<%10	n.t	3.85 ± 0.005
8c	O	2	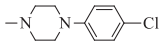	30 ± 4.2	n.t	<%10	n.t	3.95 ± 0.006
8d	O	2	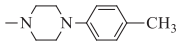	33 ± 3.7	n.t	<%10	n.t	4.03 ± 0.009
8e	O	2	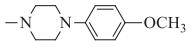	29 ± 3.3	n.t	<%10	n.t	4.28 ± 0.007
8f	O	2	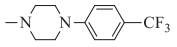	35 ± 3.2	n.t	<%10	n.t	3.90 ± 0.004
8g	O	2	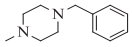	81 ± 5.2	6.94 ± 1.06	30 ± 2.6	n.t	3.78 ± 0.008
8h	O	2	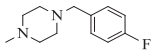	66 ± 4.3	16.10 ± 0.99	21 ± 1.8	n.t	3.92 ± 0.004
8i	O	2	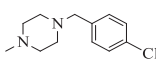	40 ± 2.1	n.t	<%10	n.t	4.19 ± 0.004
8j	O	2	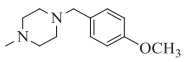	38 ± 3.2	n.t	<%10	n.t	4.20 ± 0.003
8k	O	2	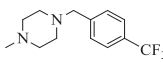	35 ± 3.5	n.t	<%10	n.t	3.96 ± 0.005
8l	O	2	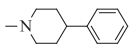	25 ± 2.7	n.t	<%10	n.t	4.09 ± 0.005
8m	O	2	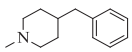	64 ± 2.3	24.60 ± 1.15	47 ± 2.6	n.t	3.87 ± 0.006
8n	O	2	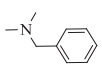	58 ± 1.1	52.40 ± 1.21	42 ± 3.5	n.t	4.30 ± 0.006
9a	S	2	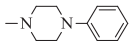	34 ± 3.0	n.t	<%10	n.t	4.24 ± 0.006
9b	S	2	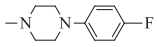	37 ± 3.2	n.t	<%10	n.t	4.03 ± 0.008
9c	S	2	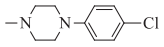	32 ± 3.4	n.t	<%10	n.t	4.43 ± 0.007
9d	S	2	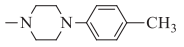	35 ± 2.8	n.t	<%10	n.t	4.31 ± 0.005
9e	S	2	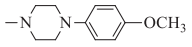	31 ± 3.0	n.t	<%10	n.t	4.55 ± 0.011
9f	S	2	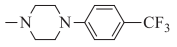	36 ± 3.1	n.t	<%10	n.t	4.10 ± 0.006
9g	S	2	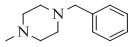	92 ± 2.4	2.34 ± 0.61	<%10	n.t	4.08 ± 0.008
9h	S	2	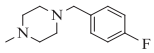	74 ± 4.1	7.09 ± 1.09	52 ± 0.9	37.60 ± 1.84	4.10 ± 0.006
9i	S	2	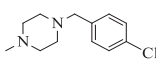	37 ± 3.2	n.t	<%10	n.t	4.01 ± 0.003
9j	S	2	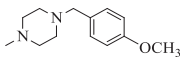	39 ± 3.4	n.t	<%10	n.t	4.28 ± 0.008
9k	S	2	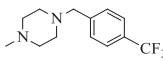	35 ± 3.7	n.t	<%10	n.t	4.45 ± 0.006

Table 1 (*continued*)

Compd	X	n	R	*ee*AChE		*eq*BChE		ORAC
				% inhibition ± SD (100 μM)	IC_{50} ± SD (μM)	% inhibition ± SD (100 μM)	IC_{50} ± SD (μM)	
9l	S	2	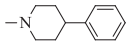	60 ± 4.1	60.30 ± 2.24	81 ± 0.8	11.14 ± 1.07	4.31 ± 0.007
9m	S	2	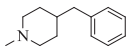	62 ± 4.6	31.90 ± 1.46	60 ± 3.3	75.38 ± 1.99	4.01 ± 0.009
9n	S	2	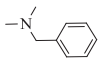	63 ± 1.3	49.50 ± 1.54	70 ± 1.5	41.96 ± 1.12	3.90 ± 0.007
10a	O	3	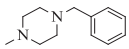	94 ± 0.2	6.00 ± 1.13	<%10	n.t	3.97 ± 0.004
10b	S	3	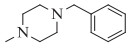	93 ± 0.3	1.96 ± 0.42	<%10	n.t	3.91 ± 0.003
10c	S	3	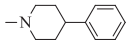	32 ± 2.1	n.t	90 ± 1.6	9.65 ± 1.13	2.93 ± 0.04
11a	O	4	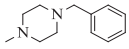	82 ± 1.0	30.86 ± 1.08	<%10	n.t	2.63 ± 0.03
11b	S	4	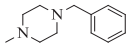	87 ± 1.7	13.96 ± 1.02	<%10	n.t	2.67 ± 0.04
11c	S	4	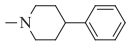	30 ± 2.3	n.t	96 ± 0.2	2.98 ± 1.02 2.56 ± 0.23[b]	2.61 ± 0.02
14a	O	_	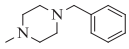	97 ± 2.3	0.89 ± 0.14	<%10	n.t	3.03 ± 0.04
14b	S	_	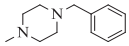	99 ± 0.6	0.34 ± 0.16 0.46 ± 0.04[a]	<%10	n.t	3.70 ± 0.04
14c	S	_	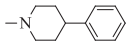	81 ± 1.2	4.32 ± 1.18	79 ± 0.4	13.97 ± 1.15	3.10 ± 0.04
21a	O	_	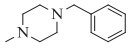	<%10	n.t	<%10	n.t	2.68 ± 0.04
21b	S	_	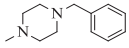	<%10	n.t	<%10	n.t	2.64 ± 0.03
Donepezil				99 ± 0.8	0.062 ± 0.002 0.048 ± 0.004[a]	88 ± 1.4	3.55 ± 0.07 6.4 ± 0.025[b]	n.t

[a] *hu*AChE.
[b] *hu*BChE, n. t: not tested.

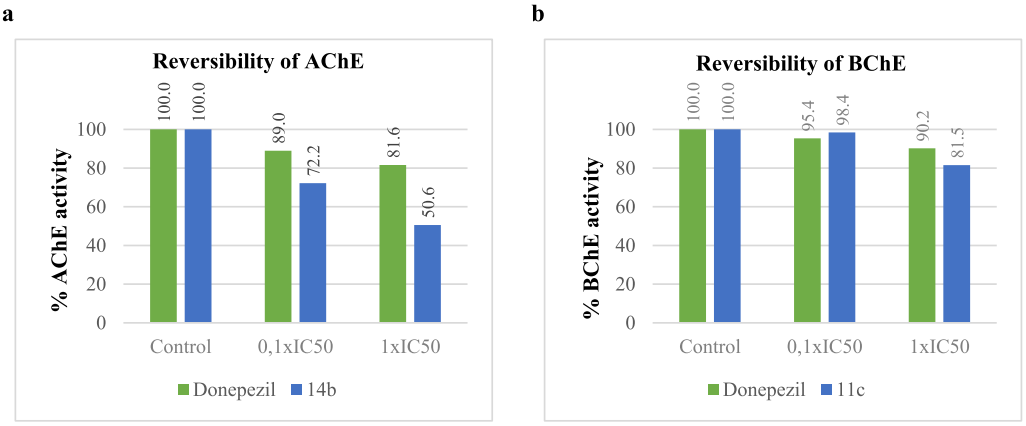

Fig. 2. Reversibility studies of compound **14b** with AChE **(a)** and compound **11c** with BChE **(b).**

Table 2
AChE and BChE reversibility studies.

	AChE		BChE	
	Donepezil	14b	Donepezil	11c
Control	100.0 ± 1.4	100.0 ± 1.4	100.0 ± 3.1	100.0 ± 3.1
$0.1xIC_{50}$	89.0 ± 0.9	72.2 ± 0.7	95.4 ± 1.2	98.4 ± 1.5
$1xIC_{50}$	81.6 ± 0.6	50.6 ± 0.7	90.2 ± 1.0	81.5 ± 0.5

Additionally, inspiring through the anti-inflammatory activity study conducted with Donepezil by Arikawa et al. we evaluated the anti-inflammatory activities of the most potent cholinesterase inhibitor compounds in the present study [38]. Thus, according to cholinesterase inhibitory activity results, the most potent 8 compounds (**8g**, **9g**, **10a**, **10b**, **10c**, **11c**, **14a**, **14b**) were selected to determine their effects on inflammatory markers IL-1β, IL-6, TNF-α, and NO. Anti-inflammatory activities of selected compounds were

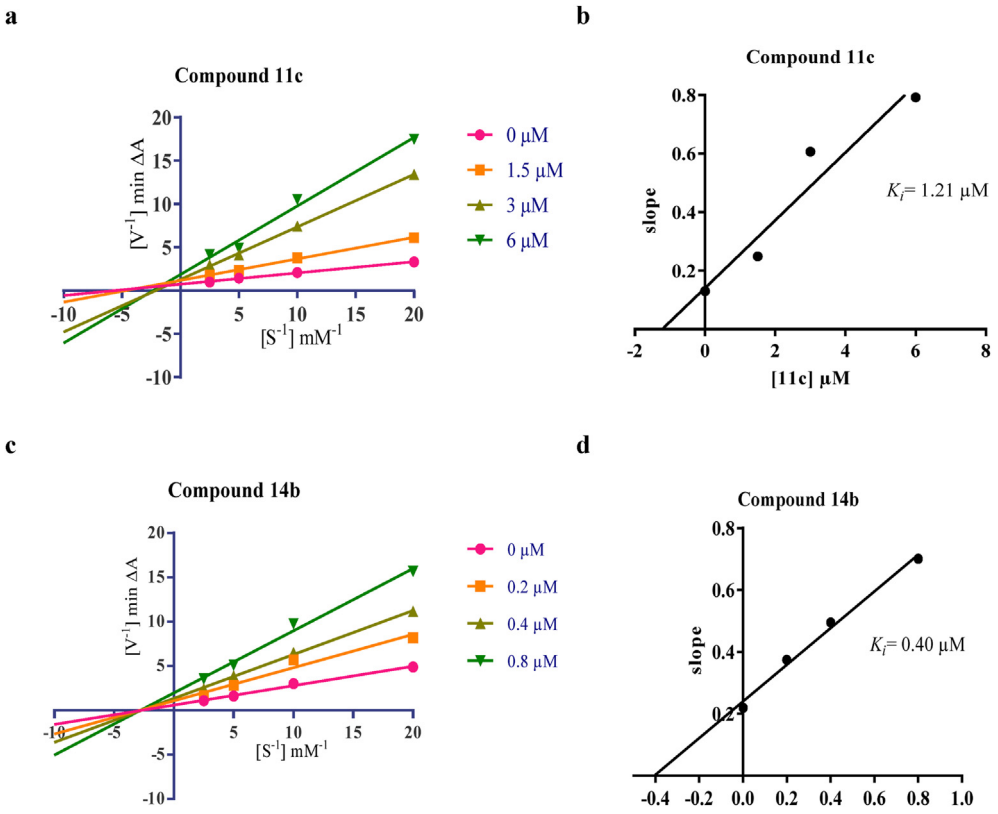

Fig. 3. Lineweaver-Burk plot of **11c** for BChE hydrolysis (**a**) and slope replot vs **11c** concentration (**b**). Lineweaver-Burk plot of **14b** for AChE hydrolysis (**c**) and slope replot vs **14b** concentration (**d**).

evaluated according to the reduction of LPS- induced IL-1β, IL-6, TNF-α, and NO production in THP 1 cell line. As seen in Fig. 4, the results revealed that the selected compounds inhibited the release of IL-1β, IL-6, and TNF-α as effectively as donepezil. Significantly, the most active AChE inhibitor, **14b** decreased NO production better than donepezil. Additionally, the other compounds inhibited NO production comparable to the effect of donepezil.

2.7. Inhibition of 11c and 14b on self-induced $A\beta_{1-42}$ aggregation

With respect to the cholinesterase inhibitory activity results, the most potent two compounds (**11c** and **14b**) were selected for Aβ aggregation inhibition assay. To investigate the effect of the selected compounds and references (curcumin and phenol red) on the aggregation of $A\beta_{1-42}$, the reported thioflavin T-based fluorometric assay was performed at 50 µM concentration. The effects of each compound on the $A\beta_{1-42}$ peptide self-aggregation was summarized as the percent (%) inhibition data in Table 3. According to the results, compounds **11c** and **14b** were found to be as active as curcumin.

2.8. Effect of 11c and 14b on apoptosis in 3T3 cells

Annexin V/PI double staining method was employed to evaluate the effects of compounds **11c** and **14b** on apoptosis in 3T3 cells at 10 µM concentration. As shown in Table 4 and Fig. 5, the results indicated that both **11c** and **14b** do not have apoptotic effects.

2.9. Cytotoxicity test

Cytotoxicity test was investigated in the 3T3 cell line to determine the safety profiles of two compounds with the best AChE (**14b**) and BChE (**11c**) inhibitory effects by using 3-(4,5-dimethylthiazol-2-yl)-2,5-diphenyltetrazolium bromide (MTT) assay. According to the results presented in Table 5, **11c** and **14b** have no significant effect on cell line at their cholinesterase inhibitor concentrations.

2.10. Assessment of physicochemical parameters

The physicochemical properties and BBB penetration scores of the selected compounds (**8g**, **9g**, **10a**, **10b**, **10c**, **11c**, **14a**, **14b**) in our study were calculated by employing Molinspiration and admetSAR online services. Calculated descriptors such as molecular weight, logP, topological polar surface area (tPSA), volume, number of hydrogen donors, number of hydrogen acceptors and number of violations of Lipinski's rule and blood brain barrier (BBB) permeability were presented in Table 6. According to the calculated data, the selected compounds have a high rate of drug-likeness because all of them following the Lipinski's rule and their predicted BBB penetration rates over % 90.

2.11. Molecular docking

Docking of the synthesized compounds was performed to predict the binding orientations and non-covalent interactions with the active sites of the AChE and BChE. In case of docking with AChE, two active compounds (**9g** and **14b**) and inactive compound (**9a**) were selected based on the experimental results on their AChE inhibitory activities. The most energetically profitable poses of these compounds in the AChE binding site were given in Fig. 6 with both three-dimensional representation and two-dimensional interaction diagram.

Aromatic amino acids Trp84 and Phe330 at the catalytic active

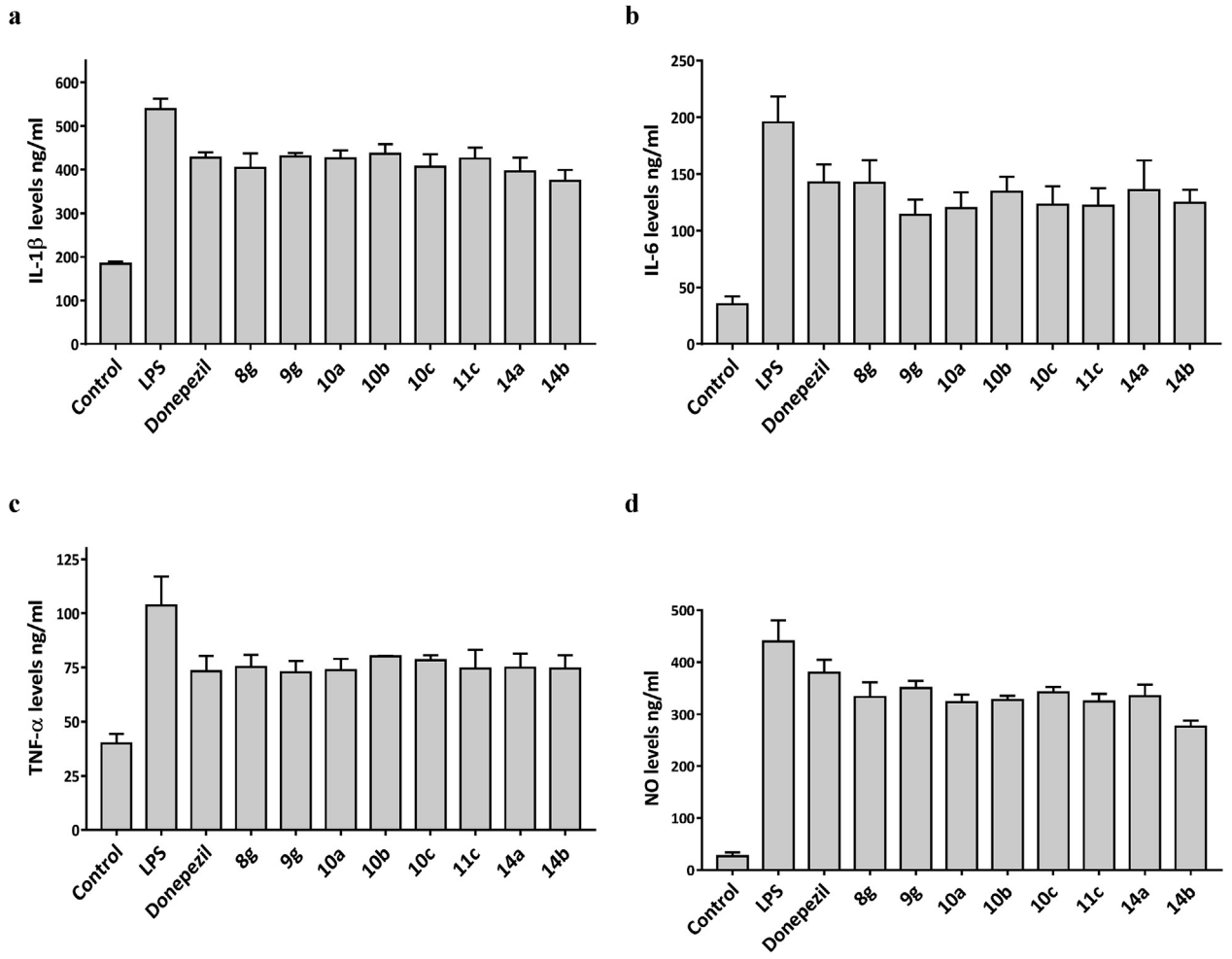

Fig. 4. The effect of donepezil and selected compounds on LPS-induced IL-1β secretion **(a).** The effect of donepezil and selected compounds on LPS-induced IL-6 secretion **(b)**. The effect of donepezil and selected compounds on LPS-induced TNF-α secretion **(c)**. The effect of donepezil and selected compounds on LPS-induced NO secretion **(d)**. ($P < 0.05$ versus control).

Table 3
Inhibition of Aβ aggregation of selected compounds.

Compound	% inhibition $A\beta_{42}$ self-aggregation ± SEM[a]
Curcumin	57.1 ± 3.0
Phenol Red	32.2 ± 0.8
11c	55.6 ± 3.7
14b	57.5 ± 5.3

[a] Inhibition of $A\beta_{42}$ self-aggregation investigated by the thioflavin-T fluorescence assay. Assays were carried out in the presence of 50 μM inhibitor and 50 μM $A\beta_{42}$ ([I] = [$A\beta_{42}$]); Data are the mean of two independent experiments each performed in triplicate.

site and Trp279 at the peripheral anionic site of AChE were reported as important residues for ligand binding affinity and specificity [39]. As seen in Fig. 6, π···π interactions with the phenyl ring of Trp84 and Trp279 and C—H···π interaction with Phe330 were characteristics for both active compounds **9g** and **14b**. For the inactive compound **9a**, π···π stacking interaction with Trp279 was conserved, while interactions with other aromatic residues Trp84 and Phe330 were missing. Inactivity of compound **9a** can be related to these missing interactions. Binding free energies obtained with docking were not significant to explain AChE inhibitory effects of compound **9a**. Other common interactions of all compounds with AChE were water-mediated contacts, hydrogen bonding interaction between Ser286 and benzothiazole sulphur, and C—H···π interactions with Phe331 and Tyr334 residues, with distances of 2.7 Å—4.4 Å. For the docking of **9g** and **14b** to AChE, binding affinity values of −10.0 and −9.8 kcal mol^{-1} were obtained, respectively with a good agreement with the experimental results. Slightly lower binding free energy value of **14b** can be attributed to the

Table 4
The effect of 11c and 14b on apoptosis in 3T3 cells. Annexin V-FITC (−)/Propidium Iodide (+): Dead cells. Annexin V-FITC (+)/Propidium Iodide (+): Late apoptotic cells. Annexin V-FITC (−)/Propidium Iodide (−): Live cells. Annexin V-FITC (+)/Propidium Iodide (−): Early apoptotic cells. Data are presented by mean ± SD in 10 μM concentration.

Compound	Annexin V-/PI+	Annexin V+/PI+	Annexin V-/PI-	Annexin V+/PI-
	% Mean ± SD			
Control	0	0.13 ± 0.06	98.83 ± 1.44	0.97 ± 1.42
11c	0.23 ± 0.15	0.33 ± 0.32	97.70 ± 1.91	1.73 ± 1.53
14b	0.40 ± 0.10	0.27 ± 0.21	98.33 ± 0.21	1.03 ± 0.40

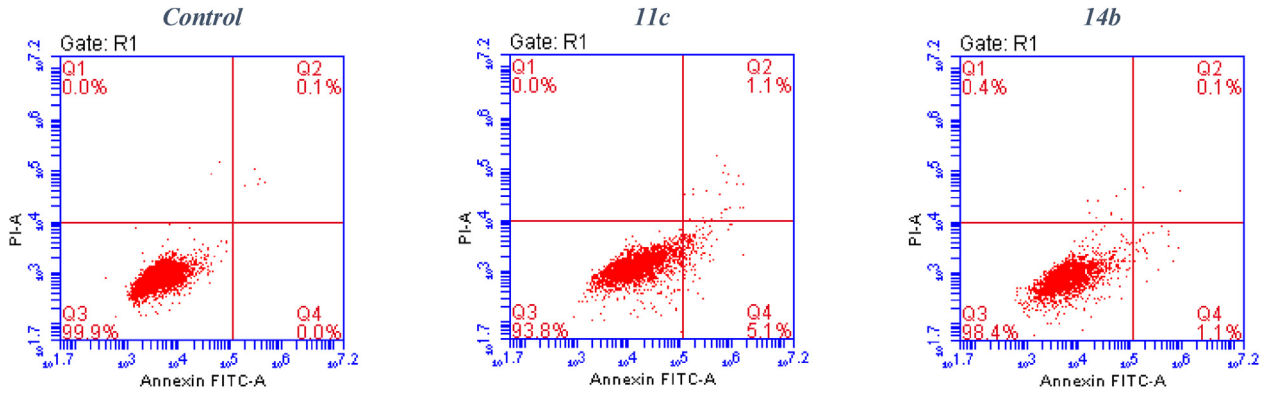

Fig. 5. The data generated by flow cytometry were plotted in two-dimensional dot plots in which PI is represented versus Annexin V-FICT. Region Q3 (Annexin V−PI−) contains the vital population, region Q4 (Annexin V + PI−) contains the early apoptotic cells, region Q1 (Annexin V-PI+) contains the dead cells and region Q2 (Annexin V + PI+) contains the late apoptotic cells.

Table 5
Cytotoxicity assay results of **11c** and **14b**.

Compound	Viability (%) of 3T3 cells		
	0.1 μM	1 μM	10 μM
11c	98.9 ± 3.8	97.1 ± 3.4	93.6 ± 0.3
14b	101.7 ± 2.9	99.3 ± 12.4	92.6 ± 10.7

Table 6
Calculated physicochemical parameters of the compounds.

Compound	MW[a]	logP[a]	tPSA[a]	nON[a]	nOHNH[a]	Vol[a]	BBB[b]	Vio[a]
8g	394,48	1,99	70,72	7	1	365,65	0,9878	0
9g	410,54	2,63	57,58	6	1	374,79	0,9919	0
10a	408,50	2,26	70,72	7	1	382,45	0,9807	0
10b	424,57	2,90	57,58	6	1	391,59	0,9903	0
10c	409,56	4,08	54,34	5	1	378,83	0,9908	0
11c	438,60	3,41	57,58	6	1	408,39	0,9908	0
14a	379,46	2,33	58,69	6	0	353,25	0,9933	0
14b	395,53	2,98	45,55	5	0	362,39	0,9939	0

MW: Molecular weight; logP: log octanol/water partition coefficient; tPSA: Total Polar Surface Area; nON: number of Hydrogen acceptors; nOHNH: number of Hydrogen donors; Vol: Molecular volume; Vio: Violation of Lipinski's rule.
[a] Calculated with Molinspiration.
[b] Calculated with admetSAR.

predicted hydrogen bonding interactions with Glu199 and Phe290 residues which were absent in case of docking with **9g**.

In Fig. 7, three-dimensional docking views and interaction diagrams were shown for the active compound **11c** and inactive compound **9a** bound to the BChE enzyme. Aromatic π···π stacking with Trp82 and C—H···π interaction with Trp231 were conserved for all these compounds, with distance range of 3.6 Å—4.3 Å. Unlike **9a**, additional stabilization by hydrogen bonding and C—H···π interactions were obtained between **11c** and BChE. It was predicted two C—H···π interactions between phenyl group of **11c** and both of Leu286 and Phe329, and two hydrogen bonding interactions between benzothiazole sulphur of 11c and Glu197 and His438 residues of BChE. Higher BChE inhibitory activity of **11c** relative to compound **9a** may be attributed to all these non-covalent interactions obtained for this.

3. Conclusion

Taking into consideration the structure activity relationships of the synthesized compounds, **14b** (IC_{50} = 0.34 μM), the keton derivative with benzothiazolone core, was the most potent and a selective inhibitor of AChE, while **11c** (IC_{50} = 2.98 μM), the pentanamide derivative with benzothiazolone core, was the most potent and a selective inhibitor of BChE. These results showed that the benzothiazolone ring was more favorable for both AChE and BChE inhibition. Moreover, it was observed that the ketone function was more suitable for AChE inhibitory activity, while the amide group was more favorable for BChE inhibitory activity. Additionally, all the tested compounds, including **11c** and **14b**, displayed good ORAC-FL values ranging from 2.61 to 4.55 fold of Trolox at 10 μM concentration. Furthermore, the selected compounds **(i.e, 8g, 9g, 10a, 10b, 10c, 11c, 14a, 14b)** had a significant effect on inflammatory markers (IL-1β, IL-6, TNF-α, NO) in LPS stimulated THP1 cells inflammation. Compounds **14b** and **11c** were not found to be statistically significantly different from donepezil in reducing LPS-induced IL-1β, IL-6 and TNF-α levels. Notably, compound **14b** was found to be better at reducing LPS-induced NO than the donepezil. Besides, **11c** and **14b** exhibited significantly $A\beta_{1\text{-}42}$ *anti*-aggregatory action as much as curcumin under our experimental condition. Meanwhile, neither **11c** nor **14b** did not show a cytotoxic or apoptotic effect. Collectively, the above-mentioned multifunctional properties highlighted **11c** and **14b** as promising potential leads for further studies.

4. Experimental

4.1. Chemistry

All the chemicals used for the synthesis of the compounds were purchased from commercial suppliers. Melting points (mp) were recorded on a Schmelzpunkt SMP-II digital melting point apparatus and values are uncorrected. Thin-layer chromatography (TLC) was performed on Merck 60F254 plates. ^{1}H (400 MHz) and ^{13}C (100 MHz) NMR spectra were recorded with a Varian Mercury 400 MHz FT-NMR spectrometer in DMSO-d_6 using tetramethylsilane as the internal standard (Faculty of Pharmacy, Ankara University). All chemical shifts were recorded as δ (ppm) and coupling constants (J) are reported as Hertz. The high-resolution mass spectra (HRMS) were obtained on a Waters LCT Premier XE Mass Spectrometer also coupled to an AQUITY Ultra Performance Liquid Chromatography system at Faculty of Pharmacy, Gazi University, Ankara, Turkey. Elemental analysis was performed on a Leco 932 CHNS instrument at the Faculty of Pharmacy, Ankara University, Ankara, Turkey, and the results were within ±0.4% of the theoretical values.

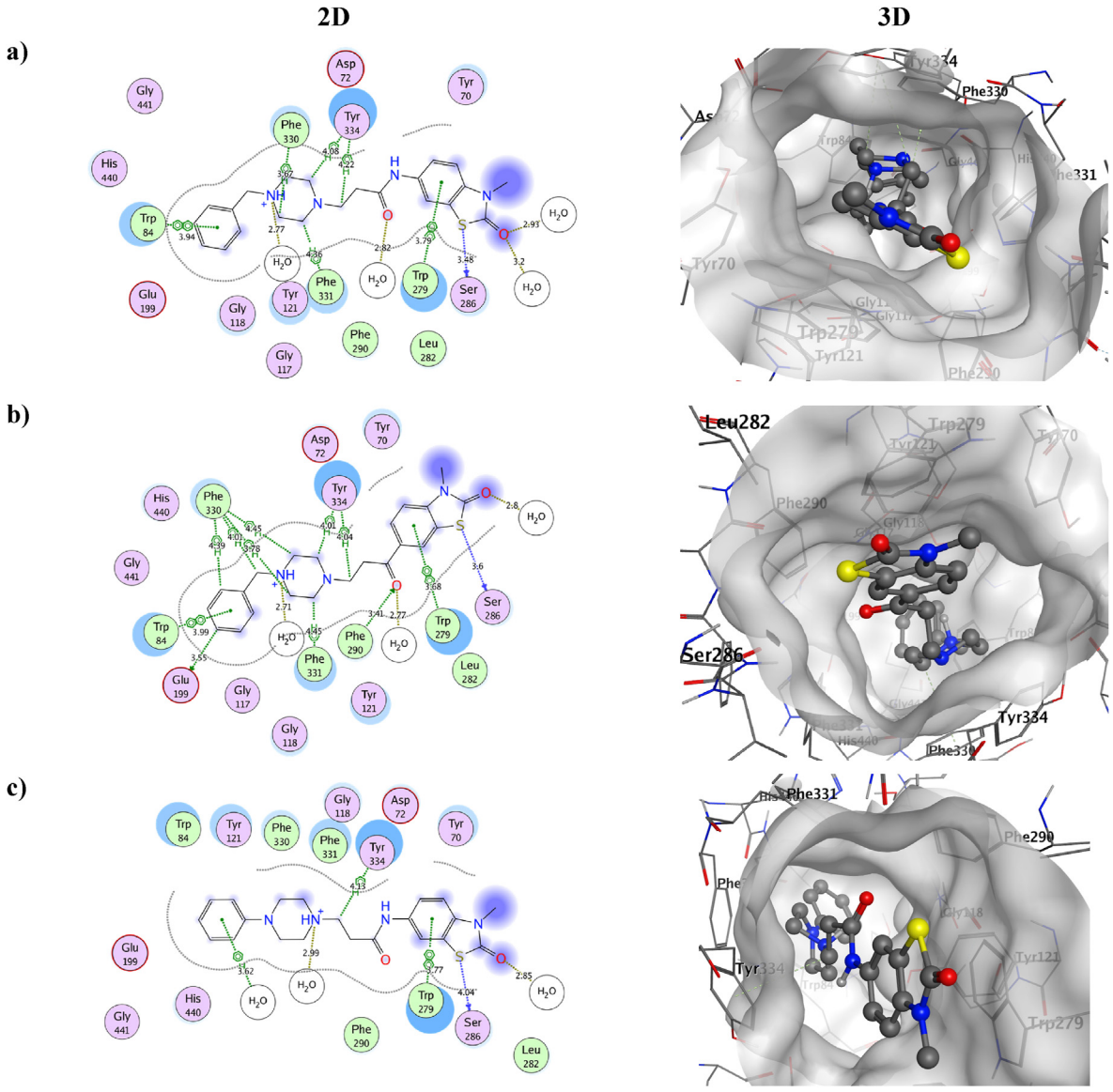

Fig. 6. 2D and 3D representation of docking poses for the compounds **9g (a), 14b (b)** and **9a (c)** in the active site of AChE (PDB code: 1EVE).

*4.1.1. 3-Methyl-2(3H)-benzoxazolone (**1**)/3-methyl-2(3H)-benzothiazolone (**2**)*

3-methyl-2(3*H*)-benzoxazolone (**1**) and 3-methyl-2(3*H*)-benzothiazolone (**2**) were synthesized according to the previously reported method. Yield for **(1)**: 80%.; mp: 84 °C. HRMS (ESI) $[M+H]^+$ *m/z* for $C_8H_7NO_2$ calculated: 150.0555, found: 155.0558. Yield for **(2)**: 90%; mp: 76 °C. HRMS (ESI) $[M+H]^+$ *m/z* for C_8H_7NOS calculated: 166.0327, found: 166.0319 [31,32].

*4.1.2. 3-Methyl-6-nitro-2(3H)-benzoxazolone (**3**)/3-methyl-6-nitro-2(3H)-benzothiazolone (**4**)*

3-methyl-6-nitro-2(3*H*)-benzoxazolone (**3**) and 3-methyl-6-nitro-2(3*H*)-benzothiazolone (**4**) were synthesized according to the previously reported method. Yield for **(3)**: 85%.; mp: 181.5 °C. HRMS (ESI) $[M+H]^+$ *m/z* for $C_8H_6N_2O_4$ calculated: 195.0406, found: 195.0410. Yield for **(4)**: 91%; mp: 164 °C. HRMS (ESI) $[M+H]^+$ *m/z* for $C_8H_6N_2O_3S$ calculated: 211.0177, found: 211.0175 [31,32].

*4.1.3. 6-Amino-3-methyl-2(3H)-benzoxazolone (**5**)/6-amino-3-methyl-2(3H)-benzothiazolone (**6**)*

6-amino-3-methyl-2(3*H*)-benzoxazolone (**5**) and 6-amino-3-methyl-2(3*H*)-benzothiazolone (**6**) were synthesized according to the previously reported method. Yield for **(5)**: 87%.; mp: 154 °C. HRMS (ESI) $[M+H]^+$ *m/z* for $C_8H_8N_2O_2$ calculated: 165.0664, found: 165.0665. Yield for **(6)**: 90%; mp: 188.5 °C. HRMS (ESI) $[M+H]^+$ *m/z* for $C_8H_8N_2OS$ calculated: 181.0436, found: 181.0440 [31,32].

*4.1.4. 3-Chloro-N-(3-methyl-2-oxo-2,3-dihydrobenzoxazol-6-yl) propanamide (**7**)*

To the solution of 500 mg (3 mmol) 6-amino-3-methyl-1,3-benzoxazole-2(3*H*)-one (**5**) in 6 ml DMF was added 37 mg (0.3 mmol) DMAP and 0.32 ml (2.2 mmol) TEA and mixed for 10 min. After reaction mixture cooled in ice bath, 0.38 ml (4 mmol) 3-chloropropionyl chloride was added and then mixed for 1 h at room temperature. At the end of this period, the reaction mixture was poured into ice water. The precipitate was filtered in vacuo,

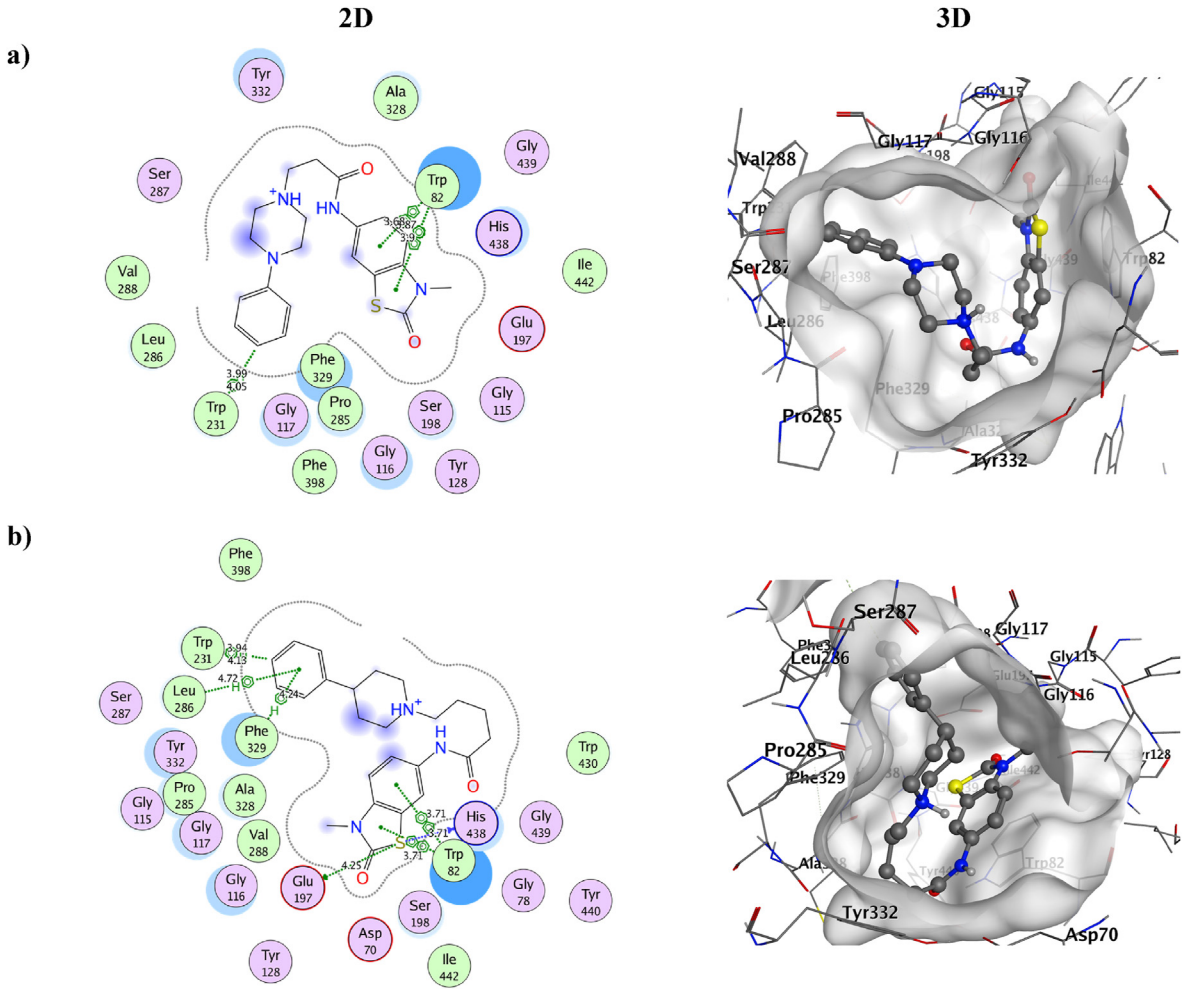

Fig. 7. 2D and 3D representation of docking pose for the compounds **9a (a)** and **11c (b)** in the active site of BChE (PDB code: 4BDS).

dried and used for the next step without further purification. Yield: 67%; mp: 204 °C (decomposed). HRMS (ESI) $[M+H]^+$ *m/z* for $C_{11}H_{11}ClN_2O_3$ calculated: 255.0536, found: 255.0529. (CAS number: 1888921-51-4).

*4.1.5. General procedure for the preparation of 3-substituted-N-(3-methyl-2-oxo-2,3-dihydro-1,3-benzoxazol-6-yl)propanamide derivatives **(8a-n)** (method A)*

NaI (3 equivalent) was added to intermediate **7** (1 equivalent) in ACN (25 ml) and mixture was refluxed for 1.5 h and cooled to room temperature. Subsequently, anhydrous potassium carbonate (2.5 equivalent) and appropriate amine derivative (2.5 equivalent) were added. Then, the mixture was refluxed for 5 h. After evaporation under reduced pressure, the crude product was purified by crystallization from an appropriate solvent.

*4.1.5.1. N-(3-methyl-2-oxo-2,3-dihydrobenzoxazol-6-yl)-3-(4-phenylpiperazin-1-yl)propanamide **(8a)**.* The intermediate **7** (382 mg, 1.5 mmol) was treated with phenylpiperazine (0.58 ml, 3.8 mmol) in the presence of NaI (675 mg, 4.5 mmol) and anhydrous potassium carbonate (525 mg, 3.8 mmol) according to method A then, it was recrystallized from ACN. Yield: 502 mg, 88%; mp: 215.9 C. ^{1}H NMR (DMSO-d_6) δ: 10.13 (s, 1H, *N*–H), 7.72 (d, 1H, J = 1.7 Hz, H^7), 7.26 (dd, 1H, J = 8.2 Hz, J = 1.7 Hz, H^5), 7.19–7.13 (m, 3H, $H^{3'}$, $H^{5'}$, H^4), 6.90 (d, 2H, J = 8.0 Hz, $H^{2'}$, $H^{6'}$), 6.74 (t, 1H, J = 8.0 Hz, $H^{4'}$), 3.28 (s, 3H, *N*–CH_3), 3.11 (t, 4H, J = 4.9 Hz, H^3, H^5-piperazine), 2.67 (t, 2H, J = 7.0 Hz, -*N*-CH_2-CH_2-), 2.55 (t, 4H, J = 4.9 Hz, H^2, H^6-piperazine), 2.48 (m, 2H, J = 7.0 Hz, -*N*–CH_2–CH_2-). ^{13}C NMR (DMSO-d_6) δ: 170.0, 154.1, 150.9, 141.7, 134.3, 128.8, 127.1, 118.7, 115.3, 114.4, 108.7, 101.4, 53.6, 52.4, 48.1, 34.1, 27.9. HRMS (ESI) $[M+H]^+$ *m/z* for $C_{21}H_{25}N_4O_3$ calculated: 381.1927, found: 381.1929. Anal. Calcd. for $C_{21}H_{24}N_4O_3$: C, 66.30; H, 6.36; N, 14.73. Found: C, 65.98; H, 6.39; N, 14.85.

*4.1.5.2. 3-[4-(4-Fluorophenyl)piperazin-1-yl]-N-(3-methyl-2-oxo-2,3-dihydrobenzoxazol-6-yl)propanamide **(8b)**.* The intermediate **7** (382 mg, 1.5 mmol) was treated with 1-(4-fluorophenyl)piperazine (685 mg, 3.8 mmol) in the presence of NaI (675 mg, 4.5 mmol) and anhydrous potassium carbonate (525 mg, 3.8 mmol) according to method A then, it was recrystallized from ACN. Yield: 537 mg, 90%; mp: 239.3 C. ^{1}H NMR (DMSO-d_6) δ: 10.12 (s, 1H, *N*–H), 7.72 (d, 1H, J = 1.7 Hz, H^7), 7.26 (dd, 1H, J = 8.3 Hz, J = 1.7 Hz, H^5), 7.14 (d, 1H, J = 8.3 Hz, H^4), 7.03–6.99 (m, 2H, $H^{3'}$, $H^{5'}$), 6.93–6.90 (m, 2H, $H^{2'}$, $H^{6'}$), 3.28 (s, 3H, *N*–CH_3), 3.05 (t, 4H, J = 4.7 Hz, H^3, H^5-piperazine), 2.67 (t, 2H, J = 7.0 Hz, -*N*-CH_2-CH_2-), 2.54 (t, 4H, J = 4.7 Hz, H^2, H^6-piperazine), 2.50–2.47 (m, 2H, -*N*–CH_2–CH_2-, with DMSO).^{13}C NMR (DMSO-d_6) δ: 169.9, 155.8 (d, J = 233.9 Hz), 154.0, 147.8, 141.6, 134.3, 127.0, 116.9 (d, J = 7.6 Hz), 115.1 (d, J = 21.4 Hz), 114.3, 108.6, 101.4, 53.5, 52.3, 48.8, 34.0, 27.9. HRMS (ESI) $[M+H]^+$ *m/z* for $C_{21}H_{24}FN_4O_3$ calculated: 399.1832, found: 399.1837. Anal. Calcd. for $C_{21}H_{23}FN_4O_3$: C, 62.90; H, 5.82; N, 14.06. Found: C, 62.54; H, 5.99; N, 14.06.

*4.1.5.3. 3-[4-(4-Chlorophenyl)piperazin-1-yl]-N-(3-methyl-2-oxo-2,3-dihydrobenzoxazol-6-yl)propanamide **(8c)**.* The intermediate **7** (382 mg, 1.5 mmol) was treated with 1-(4-chlorophenyl)piperazine (747 mg, 3.8 mmol) in the presence of NaI (675 mg, 4.5 mmol) and anhydrous potassium carbonate (525 mg, 3.8 mmol) according to method A then, it was recrystallized from butanol. Yield: 454 mg, 73%; mp: 249.7 C. ^{1}H NMR (DMSO-d_6) δ: 10.11 (s, 1H, *N*—H), 7.72 (s, 1H, H^7), 7.26 (d, 1H, J = 8.2 Hz, H^5), 7.19 (d, 2H, J = 9.0 Hz, $H^{3'}$, $H^{5'}$), 7.14 (d, 1H, J = 8.2 Hz, H^4), 6.91 (d, 2H, J = 9.0 Hz, $H^{2'}$, $H^{6'}$), 3.31 (s, 3H, *N*—CH_3), 3.10 (bt, 4H, H^3, H^5-piperazine), 2.66 (t, 2H, J = 7.0 Hz, -*N*-CH_2-CH_2-), 2.53 (bt, 4H, H^2, H^6-piperazine), 2.50—2.46 (m, 2H, -*N*—CH_2—CH_2-, with DMSO). ^{13}C NMR (DMSO-d_6) δ: 169.9, 154.0, 149.6, 141.6, 134.2, 128.4, 127.0, 122.1, 116.6, 114.3, 108.6, 101.4, 53.5, 52.1, 47.9, 34.0, 27.9. HRMS (ESI) $[M+H]^+$ m/z for $C_{21}H_{24}ClN_4O_3$ calculated: 415.1537, found: 415.1539. Anal. Calcd. for $C_{21}H_{23}ClN_4O_3$: C, 58.68; H, 5.59; N, 13.10. Found: C, 58.28; H, 5.92; N, 12.97.

*4.1.5.4. 3-[4-(4-Methylphenyl)piperazin-1-yl]-N-(3-methyl-2-oxo-2,3-dihydrobenzoxazol-6-yl)propanamide **(8d)**.* The intermediate **7** (382 mg, 1.5 mmol) was treated with 1-(4-methylphenyl)piperazine (670 mg, 3.8 mmol) in the presence of NaI (675 mg, 4.5 mmol) and anhydrous potassium carbonate (525 mg, 3.8 mmol) according to method A then, it was recrystallized from ethanol. Yield: 473 mg, 80%; mp: 244 °C. ^{1}H NMR (DMSO-d_6) δ: 10.14 (s, 1H, *N*—H), 7.74 (d, 1H, J = 2.0 Hz, H^7), 7.28 (dd, 1H, J = 8.5 Hz, J = 2.0 Hz, H^5), 7.16 (d, 1H, J = 8.5 Hz, H^4), 7.01 (d, 2H, J = 8.6 Hz, $H^{3'}$, $H^{5'}$), 6.82 (d, 2H, J = 8.6 Hz, $H^{2'}$, $H^{6'}$), 3.31 (s, 3H, *N*—CH_3), 3.06 (t, 4H, J = 4.9 Hz, H^3, H^5-piperazine), 2.68 (t, 2H, J = 7.0 Hz, -*N*-CH_2-CH_2-), 2.56 (t, 4H, J = 4.9 Hz, H^2, H^6-piperazine), 2.52—2.49 (m, 2H, -*N*—CH_2—CH_2-, with DMSO), 2.19 (s, 3H, phenyl-CH_3). ^{13}C NMR (DMSO-d_6) δ: 169.9, 154.0, 148.8, 141.6, 134.3, 129.2, 127.4, 127.0, 115.5, 114.3, 108.7, 101.4, 53.6, 52.3, 48.6, 34.0, 27.9, 19.9. HRMS (ESI) [M+H]+ m/z for $C_{22}H_{27}N_4O_3$ calculated: 395.2083, found: 395.2083. Anal. Calcd. for $C_{22}H_{26}N_4O_3.0.5C_2H_5OH$: C, 66.16; H, 7.00; N, 13.41. Found: C, 65.76; H, 7.05; N, 13.42.

*4.1.5.5. 3-[4-(4-Methoxyphenyl)piperazin-1-yl]-N-(3-methyl-2-oxo-2,3-dihydrobenzoxazol-6-yl)propanamide **(8e)**.* The intermediate **7** (382 mg, 1.5 mmol) was treated with 1-(4-methoxyphenyl)piperazine (730 mg, 3.8 mmol) in the presence of NaI (675 mg, 4.5 mmol) and anhydrous potassium carbonate (525 mg, 3.8 mmol) according to method A then, it was recrystallized from ethanol. Yield: 498 mg, 81%; mp: 214.7 C. ^{1}H NMR (DMSO-d_6) δ: 10.12 (s, 1H, *N*—H), 7.71 (d, 1H, J = 2.0 Hz, H^7), 7.26 (dd, 1H, J = 8.4 Hz, J = 2.0 Hz, H^5), 7.14 (d, 1H, J = 8.4 Hz, H^4), 6.86 (d, 2H, J = 9.0 Hz, $H^{3'}$, $H^{5'}$), 6.78 (d, 2H, J = 9.0 Hz, $H^{2'}$, $H^{6'}$), 3.65 (s, 3H, *O*—CH_3), 3.29 (s, 3H, *N*—CH_3), 2.99 (t, 4H, J = 4.7 Hz, H^3,H^5-piperazine), 2.66 (t, 2H, J = 7.0 Hz, -*N*-CH_2-CH_2-), 2.54 (t, 4H, J = 4.8 Hz, H^2,H^6-piperazine), 2.49—2.46 (m, 2H, J = 7.0 Hz, -*N*—CH_2—CH_2-, with DMSO).^{13}C NMR (DMSO-d_6) δ: 169.9, 154.0, 152.7, 145.3, 141.6, 134.3, 127.0, 117.1, 114.3, 114.1, 108.6, 101.4, 55.0, 53.6, 52.4, 49.5, 34.0, 27.9. HRMS (ESI) $[M+H]^+$ m/z for $C_{22}H_{27}N_4O_4$ calculated: 411.2032, found: 411.2028. Anal. Calcd. for $C_{22}H_{26}N_4O_4 \cdot 1H_2O$: C, 61.66; H, 6.58; N, 13.07. Found: C, 61.77; H, 6.68; N, 13.17.

*4.1.5.6. 3-[4-(4-Trifluoromethylphenyl)piperazin-1-yl]-N-(3-methyl-2-oxo-2,3-dihydrobenzoxazol-6-yl)propanamide **(8f)**.* The intermediate **7** (382 mg, 1.5 mmol) was treated with 1-(4-trifluoromethylphenyl)piperazine (875 mg, 3.8 mmol) in the presence of NaI (675 mg, 4.5 mmol) and anhydrous potassium carbonate (525 mg, 3.8 mmol) according to method A then, it was recrystallized from butanol. Yield: 255 mg, 38%; mp: 257 C. ^{1}H NMR (DMSO-d_6) δ: 10.10 (s, 1H, *N*—H), 7.72 (d, 1H, J = 1.7 Hz, H^7), 7.47 (d, 2H, J = 8.8 Hz, $H^{3'}$, $H^{5'}$), 7.27 (dd, 1H, J = 8.3 Hz, J = 1.7 Hz, H^5), 7.14 (d, 1H, J = 8.3 Hz, H^4), 7.04 (d, 2H, J = 8.8 Hz, $H^{2'}$, $H^{6'}$), 3.31 (s, 3H, *N*—CH_3), 3.25 (t, 4H, J = 4.9 Hz, H^3, H^5-piperazine), 2.67 (t, 2H, J = 7.0 Hz, -*N*-CH_2-CH_2-), 2.54 (t, 4H, J = 4.9 Hz, H^2, H^6-piperazine), 2.51—2.47 (m, 2H, -*N*—CH_2—CH_2-, with DMSO). ^{13}C NMR (DMSO-d_6) δ: 169.8, 154.0, 153.1, 141.6, 134.2, 127.1, 125.9 (q, J = 3.9 Hz), 124.8 (q, J = 269.0 Hz), 117.7 (q, J = 31.7), 114.4, 114.0, 108.6, 101.5, 53.5, 52.0, 46.9, 34.0, 27.8. HRMS (ESI) $[M+H]^+$ m/z for $C_{22}H_{24}F_3N_4O_3$ calculated: 449.1801, found: 449.1801. Anal. Calcd. for $C_{22}H_{23}F_3N_4O_3$: C, 58.79; H, 5.17; N, 12.49. Found: C, 58.39; H, 4.95; N, 12.67.

*4.1.5.7. 3-(4-Benzylpiperazin-1-yl)-N-(3-methyl-2-oxo-2,3-dihydrobenzoxazol-6-yl)propanamide **(8g)**.* The intermediate **7** (382 mg, 1.5 mmol) was treated with 1-benzylpiperazine (670 mg, 3.8 mmol) in the presence of NaI (675 mg, 4.5 mmol) and anhydrous potassium carbonate (525 mg, 3.8 mmol) according to method A then, it was recrystallized from ACN. Yield: 414 mg, 70%; mp: 183.5 C. ^{1}H NMR (DMSO-d_6) δ: 10.12 (s, 1H, *N*—H), 7.69 (d, 1H, J = 2 0.0 Hz, H^7), 7.31—7.19 (m, 6H, H^5, phenyl protons), 7.14 (d, 1H, J = 8.4 Hz, H^4), 3.42 (s, 2H, —CH_2- C_6H_5), 3.29 (s, 3H, *N*—CH_3), 2.59 (t, 2H, J = 7.2 Hz, -*N*-CH_2-CH_2-), 2.43 (t, 2H, J = 7.2 Hz, -*N*—CH_2—CH_2-), 2.41—2.35 (m, 8H, piperazine).^{13}C NMR (DMSO-d_6) δ: 169.9, 154.0, 141.7, 138.1, 134.3, 128.7, 128.0, 127.1, 126.7, 114.3, 108.7, 101.4, 61.9, 53.6, 52.5, 52.4, 34.0, 27.9. HRMS (ESI) $[M+H]^+$ m/z for $C_{22}H_{27}N_4O_3$ calculated: 395.2083, found: 395.2083. Anal. Calcd. for $C_{22}H_{26}N_4O_3$: C, 66.99; H, 6.64; N, 14.20. Found: C, 66.86; H, 6.64; N, 14.15.

*4.1.5.8. 3-[4-(4-Fluorobenzyl)piperazin-1-yl]-N-(3-methyl-2-oxo-2,3-dihydrobenzoxazol-6-yl)propanamide **(8h)**.* The intermediate **7** (382 mg, 1.5 mmol) was treated with 1-(4-fluorobenzyl)piperazine (737 mg, 3.8 mmol) in the presence of NaI (675 mg, 4.5 mmol) and anhydrous potassium carbonate (525 mg, 3.8 mmol) according to method A then, it was recrystallized from butanol. Yield: 457 mg, 74%; mp: 164.2 C. ^{1}H NMR (DMSO-d_6) δ: 10.12 (s, 1H, *N*—H), 7.69 (d, 1H, J = 2.0 Hz, H^7), 7.31—7.23 (m, 3H, $H^{2'}$, $H^{6'}$, H^5), 7.15—7.08 (m, 3H, $H^{3'}$, $H^{5'}$, H^4), 3.41 (s, 2H, —CH_2-C_6H_5) 3.29 (s, 3H, *N*—CH_3), 2.59 (t, 2H, J = 7.0 Hz, -*N*-CH_2-CH_2-), 2.42 (t, 2H, J = 7.0 Hz, -*N*—CH_2—CH_2-), 2.40—2.30 (m, 8H, piperazine). ^{13}C NMR (DMSO-d_6) δ: 169.9, 161.1 (d, J = 240.8 Hz), 154.0, 141.6, 134.3 (d, J = 2.3 Hz), 134.2, 130.5 (d, J = 8.4 Hz), 127.0, 114.7 (d, J = 20.5 Hz), 114.3, 108.6, 101.4, 60.9, 53.6, 52.4, 52.3, 33.9, 27.9. HRMS (ESI) $[M+H]^+$ m/z for $C_{22}H_{26}FN_4O_3$ calculated: 413.1989, found: 413.1986. Anal. Calcd. for $C_{22}H_{25}FN_4O_3$: C, 64.06; H, 6.16; N, 13.43. Found: C, 63.62; H, 6.15; N, 13.50.

*4.1.5.9. 3-[4-(4-Chlorobenzyl)piperazin-1-yl]-N-(3-methyl-2-oxo-2,3-dihydrobenzoxazol-6-yl)propanamide **(8i)**.* The intermediate **7** (382 mg, 1.5 mmol) was treated with 1-(4-chlorobenzyl)piperazine (0.7 ml, 3.8 mmol) in the presence of NaI (675 mg, 4.5 mmol) and anhydrous potassium carbonate (525 mg, 3.8 mmol) according to method A then, it was recrystallized from methanol. Yield: 437 mg, 68%; mp: 170 C. ^{1}H NMR (DMSO-d_6) δ: 10.11 (s, 1H, *N*—H), 7.71 (d, 1H, J = 1.6 Hz, H^7), 7.36 (d, 2H, J = 8.4 Hz, $H^{2'}$, $H^{6'}$), 7.30 (d, 2H, J = 8.4 Hz, $H^{3'}$, $H^{5'}$), 7.26 (dd, 1H, J = 8.4 Hz, J = 1.6 Hz, H^5), 7.15 (d, 1H, J = 8.4 Hz, H^4), 3.44 (s, 2H, —CH_2-C_6H_5), 3.31 (s, 3H, *N*—CH_3), 2.62 (t, 2H, J = 7.2 Hz, -*N*-CH_2-CH_2-), 2.44 (t, 2H, J = 7.2 Hz, -*N*—CH_2—CH_2-), 2.42—2.32 (m, 8H, piperazine).^{13}C NMR (DMSO-d_6) δ: 169.9, 154.0, 141.7, 137.2, 134.3, 131.3, 130.4, 128.0, 127.0, 114.3, 108.7, 101.4, 61.0, 53.6, 52.5, 52.3, 34.0, 27.9. HRMS (ESI) $[M+H]^+$ m/z for $C_{22}H_{26}ClN_4O_3$ calculated: 429.1693, found: 429.1693. Anal. Calcd. for $C_{22}H_{25}ClN_4O_3$: C, 60.33; H, 5.98; N, 12.79. Found: C, 60.29; H, 6.13; N, 12.79.

*4.1.5.10. 3-[4-(4-Methoxybenzyl)piperazin-1-yl]-N-(3-methyl-2-oxo-2,3-dihydrobenzoxazol-6-yl)propanamide **(8j)**.* The intermediate **7** (382 mg, 1.5 mmol) was treated with 1-(4-methoxybenzyl)piperazine (784 mg, 3.8 mmol) in the presence of NaI (675 mg, 4.5 mmol)

and anhydrous potassium carbonate (525 mg, 3.8 mmol) according to method A then, it was recrystallized from ethanol. Yield: 216 mg, 34%; mp: 168.7 C. ^{1}H NMR (DMSO-d_6) δ: 10.12 (s, 1H, *N*–H), 7.70 (d, 1H, J = 1.6 Hz, H^7), 7.26 (dd, 1H, J = 8.4 Hz, J = 1.6 Hz, H^5), 7.18 (d, 2H, J = 8.2 Hz, H$^{2'}$, H$^{6'}$), 7.14 (d, 1H, J = 8.4 Hz, H^4), 6.86 (d, 2H, J = 8.2 Hz, H$^{3'}$, H$^{5'}$), 3.73 (s, 3H, *O*–CH_3), 3.37 (s, 2H, –CH_2-C_6H_5), 3.31 (s, 3H, *N*–CH_3), 2.61 (t, 2H, J = 7.0 Hz, -*N*-C$\underline{H_2}$-CH_2-), 2.44 (t, 2H, J = 7.0 Hz, -*N*–CH_2–C$\underline{H_2}$-), 2.42–2.32 (m, 8H, piperazine). ^{13}C NMR (DMSO-d_6) δ: 170.4, 158.6, 154.5, 142.2, 134.8, 130.4, 127.5, 114.8, 113.9, 109.2, 101.9, 61.8, 55.4, 54.1, 52.9, 52.9, 34.5, 28.4. HRMS (ESI) [M+H]$^+$ *m/z* for $C_{23}H_{29}N_4O_4$ calculated: 425.2189, found: 425.2189. Anal. Calcd. for $C_{23}H_{28}N_4O_4$: C, 64.39; H, 6.69; N, 13.05. Found: C, 64.42; H, 6.47; N, 13.22.

4.1.5.11. 3-[4-(4-Trifluoromethylbenzyl)piperazin-1-yl]-N-(3-methyl-2-oxo-2,3-dihydrobenzoxazol-6-yl)propanamide ***(8k)****.* The intermediate **7** (382 mg, 1.5 mmol) was treated with 1-(4-trifluoromethylbenzyl)piperazine (0.75 ml, 3.8 mmol) in the presence of NaI (675 mg, 4.5 mmol) and anhydrous potassium carbonate (525 mg, 3.8 mmol) according to method A then, it was recrystallized from 2-propanol. Yield: 451 mg, 65%; mp: 163.8 C. ^{1}H NMR (DMSO-d_6) δ: 10.15 (s, 1H, *N*–H), 7.69 (d, 1H, J = 2.0 Hz, H^7), 7.65 (d, 2H, J = 8.2 Hz, H$^{3'}$, H$^{5'}$), 7.49 (d, 2H, J = 8.4 Hz, H$^{2'}$, H$^{6'}$), 7.24 (dd, 1H, J = 8.7 Hz, J = 2.0 Hz, H^5), 7.14 (d, 1H, J = 8.7 Hz, H^4), 3.55 (s, 2H, –CH_2-C_6H_5), 3.31 (s, 3H, *N*–CH_3), 2.63 (t, 2H, J = 7.0 Hz, -*N*-C$\underline{H_2}$-CH_2-), 2.45 (t, 2H, J = 7 Hz, -*N*–CH_2–C$\underline{H_2}$-), 2.43–2.38 (m, 8H, piperazin). ^{13}C NMR (DMSO-d_6) δ: 169.9, 154.0, 141.6, 134.3, 129.2, 127.4 (q, J = 31.4 Hz), 127.0, 125.6, 124.3 (q, J = 3.6 Hz), 124.2 (q, J = 269.9 Hz), 114.3, 108.6, 101.4, 61.1, 53.6, 52.4, 52.3, 34.0, 27.9. HRMS (ESI) [M+H]$^+$ *m/z* for $C_{23}H_{26}F_3N_4O_3$ calculated: 463.1957, found: 463.1957. Anal. Calcd. for $C_{23}H_{25}F_3N_4O_3$: C, 59.73; H, 5.45; N, 12.11. Found: C, 59.39; H, 5.73; N, 12.08.

4.1.5.12. 3-(4-Phenylpiperidin-1-yl)-N-(3-methyl-2-oxo-2,3-dihydrobenzoxazol-6-yl)propanamide ***(8l)****.* The intermediate **7** (382 mg, 1.5 mmol) was treated with 4-phenylpiperidine (612 mg, 3.8 mmol) in the presence of NaI (675 mg, 4.5 mmol) and anhydrous potassium carbonate (525 mg, 3.8 mmol) according to method A then, it was recrystallized from methanol. Yield: 472 mg, 83%; mp: 171.2 C. ^{1}H NMR (DMSO-d_6) δ: 10.15 (s, 1H, *N*–H), 7.72 (d, 1H, J = 2.0 Hz, H^7), 7.28–7.14 (m, 7H, H^4, H^5, phenyl protons), 3.29 (s, 3H, *N*–CH_3), 2.98 (d, 2H, J = 11.2 Hz, H^{2e}, H^{6e}-piperidine), 2.65 (t, 2H, J = 7.2 Hz, -*N*-C$\underline{H_2}$-CH_2-), 2.49–2.43 (m, 3H, H^4-piperidine, -*N*–CH_2–C$\underline{H_2}$-, with DMSO), 2.05 (td, 2H, J = 11.2 Hz, J = 2.0 Hz, H^{2a}, H^{6a}-piperidine, 1.75–1.59 (m, 4H, H^3, H^5-piperidine).^{13}C NMR (DMSO-d_6) δ: 170.0, 154.0, 146.1, 141.7, 134.3, 128.2, 127.0, 126.5, 125.8, 114.3, 108.7, 101.4, 53.9, 53.4, 41.7, 34.1, 33.0, 27.9. HRMS (ESI) [M+H]$^+$ *m/z* for $C_{22}H_{26}N_3O_3$ calculated: 380.1974, found: 380.1973. Anal. Calcd. for $C_{22}H_{25}N_3O_3$: C, 69.64; H, 6.64; N, 11.07. Found: C, 69.51; H, 6.62; N, 11.26.

4.1.5.13. 3-(4-Benzylpiperidin-1-yl)-N-(3-methyl-2-oxo-2,3-dihydrobenzoxazol-6-yl)propanamide ***(8m)****.* The intermediate **7** (382 mg, 1.5 mmol) was treated with 4-benzylpiperidine (612 mg, 3.8 mmol) in the presence of NaI (675 mg, 4.5 mmol) and anhydrous potassium carbonate (525 mg, 3.8 mmol) according to method A then, it was recrystallized from ethanol. Yield: 312 mg, 53%; mp: 164.1 C. ^{1}H NMR (DMSO-d_6) δ: 10.16 (s, 1H, *N*–H), 7.69 (d, 1H, J = 2 Hz, H^7), 7.26–7.12 (m, 7H, H^4, H^5, phenyl protons), 3.29 (s, 3H, *N*–CH_3), 2.83 (d, 2H, J = 10.8 Hz, H^{2e}, H^{6e}-piperidin), 2.56 (t, 2H, J = 7 Hz, -*N*-C$\underline{H_2}$-CH_2-), 2.47 (m, 2H, –CH_2-C_6H_5, with DMSO), 2.41 (t, 2H, J = 7.0 Hz, -*N*–CH_2–C$\underline{H_2}$-), 1.86 (t, 2H, J = 10.8 Hz, H^{2a}, H^{6a}-piperidin), 1.53–1.45 (m, 3H, H^{3e}, H^{5e}, H^4-piperidin), 1.18–1.13 (m, 2H, H^{3a}, H^{5a}-piperidin).^{13}C NMR (DMSO-d_6) δ: 170.0, 154.0, 141.6, 140.2, 134.3, 128.8, 127.9, 127.0, 125.6, 114.3, 108.6, 101.3, 53.9, 52.8, 42.2, 37.2, 34.1, 31.6, 27.9. HRMS (ESI) [M+H]$^+$ *m/z* for $C_{23}H_{28}N_3O_3$ calculated: 394.2131, found: 394.2130. Anal. Calcd. for $C_{23}H_{27}N_3O_3$: C, 70.21; H, 6.92; N, 10.68. Found: C, 69.91; H, 6.86; N, 10.85.

4.1.5.14. 3-[Benzyl(methyl)amino]-N-(3-methyl-2-oxo-2,3-dihydrobenzoxazol-6-yl)propanamide ***(8n)****.* The intermediate **7** (382 mg, 1.5 mmol) was treated with *N*-benzyl(methyl)amine (0.49 ml, 3.8 mmol) in the presence of NaI (675 mg, 4.5 mmol) and anhydrous potassium carbonate (525 mg, 3.8 mmol) according to method A then, it was recrystallized from 2-propanol. Yield: 264 mg, 52%; mp: 165.5 C. ^{1}H NMR (DMSO-d_6) δ: 10.05 (s, 1H, *N*–H), 7.69 (s, 1H, H^7), 7.28–7.20 (m, 6H, H^5, phenyl protons), 7.14 (d, 1H, J = 8.0 Hz, H^4), 3.51 (s, 2H, –CH_2-C_6H_5), 3.29 (s, 3H, *N*–CH_3), 2.70 (t, 2H, J = 6.8 Hz, -*N*-C$\underline{H_2}$-CH_2-), 2.49 (t, 2H, J = 6.8 Hz, -*N*–CH_2–C$\underline{H_2}$-), 2.15 (s, 3H, N_2–CH_3).^{13}C NMR (DMSO-d_6) δ: 170.0, 154.1, 141.7, 134.3, 128.7, 128.0, 127.1, 126.8, 114.4, 108.7, 101.5, 60.9, 52.8, 41.5, 34.5, 27.9. HRMS (ESI) [M+H]$^+$ *m/z* for $C_{19}H_{22}N_3O_3$ calculated: 340.1661, found: 340.1662. Anal. Calcd. for $C_{19}H_{21}N_3O_3$: C, 67.24; H, 6.24; N, 12.38. Found: C, 66.84; H, 6.47; N, 12.40.

4.1.6. General procedure for the preparation of 3-substitutedpropanoic acid intermediates

A mixture of appropriate amine derivatives (1 equivalent) and methyl acrylate (1.2 equivalent) in 15 ml DCM were stirred at room temperature overnight. After completion of reaction, solvent was evaporated under reduced pressure and corresponding methyl ester was produced. To obtain desired propanoic acid, methyl ester hydrolyzed by heating at 40 °C for 2 h with 5% NaOH solution. End of this period, reaction mixture was cooled to room temperature and neutralized with HCl. The resulting precipitate was filtered, dried and used for the method B without further purification [29].

4.1.7. General procedure for the preparation of 3-substituted-N-(3-methyl-2-oxo-2,3-dihydro-1,3-benzothiazol-6-yl)propanamide derivatives ***(9a-n)*** *(method B)*

To a solution of appropriate 3-substitutedpropanoic acid (1.1 equivalent) in DCM (20 ml), EDC (1.2 equivalent), DMAP (0.2 equivalent) and intermediate **6** (1 equivalent) were added respectively in 20 min. The reaction was carried out at room temperature overnight then, the reaction mixture was evaporated to dryness. The precipitate was poured into water, filtered, and crystallized from appropriate solvent.

4.1.7.1. N-(3-methyl-2-oxo-2,3-dihydrobenzothiazol-6-yl)-3-(4-phenylpiperazin-1-yl)propanamide ***(9a)****.* Compound **9a** was obtained by using method B from intermediate **6** (360 mg, 2 mmol), 3-(4-phenylpiperazin-1-yl)propanoic acid (515 mg, 2.2 mmol), EDC (460 mg, 2.4 mmol) and DMAP (49 mg, 0.4 mmol). Then it was recrystallized from methanol. Yield: 476 mg, 60%; mp: 178.6 C. ^{1}H NMR (DMSO-d_6) δ: 10.14 (s, 1H, *N*–H), 7.95 (s, 1H, H^7), 7.45 (dd, 1H, J = 8.7 Hz, J = 1.6 Hz, H^5), 7.21 (d, 1H, J = 8.7 Hz, H^4), 7.18 (t, 2H, J = 7.6 Hz, H$^{3'}$, H$^{5'}$), 6.90 (d, 2H, J = 7.6 Hz, H$^{2'}$, H$^{6'}$), 6.74 (t, 1H, J = 7.6 Hz, H$^{4'}$), 3.35 (s, 3H, *N*–CH_3), 3.10 (m, 4H, H^3, H^5-piperazine), 2.67 (t, 2H, J = 6.8 Hz, -*N*-C$\underline{H_2}$-CH_2-), 2.55 (m, 4H, H^2, H^6-piperazine), 2.52–2.46 (m, 2H, -*N*–CH_2–C$\underline{H_2}$-, with DMSO). ^{13}C NMR (DMSO-d_6) δ: 170.0, 168.4, 150.9, 134.8, 133.2, 128.8, 121.5, 118.7, 117.9, 115.3, 113.3, 111.2, 53.7, 52.4, 48.1, 34.0, 28.9. HRMS (ESI) [M+H]$^+$ *m/z* for $C_{21}H_{25}N_4O_2S$ calculated: 397.1698, found: 397.1702. Anal. Calcd. for $C_{21}H_{24}N_4O_2S$: C, 63.61; H, 6.10; N, 14.13; S, 8.09. Found: C, 63.40; H, 6.04; N, 13.91; S, 7.99.

4.1.7.2. 3-[4-(4-Fluorophenyl)piperazin-1-yl]-N-(3-methyl-2-oxo-2,3-dihydrobenzothiazol-6-yl)propanamide ***(9b)****.* Compound **9b** was obtained by using method B from intermediate **6** (360 mg, 2 mmol), 3-[4-(4-fluorophenyl)piperazin-1-yl]propanoic acid (555 mg,

2.2 mmol), EDC (460 mg, 2.4 mmol) and DMAP (49 mg, 0.4 mmol). Then it was recrystallized from butanol. Yield: 588 mg, 71%; mp: 176.4 C. ^{1}H NMR (DMSO-d_6) δ: 10.13 (s, 1H, *N*–H), 7.94 (d, 1H, J = 1.7 Hz, H^7), 7.45 (dd, 1H, J = 8.7 Hz, J = 1.7 Hz, H^5), 7.21 (d, 1H, J = 8.7 Hz, H^4), 7.03–6.99 (m, 2H, H$^{3'}$, H$^{5'}$), 6.93–6.89 (m, 2H, H$^{2'}$, H$^{6'}$), 3.35 (s, 3H, *N*–CH_3), 3.05 (t, 4H, J = 4.8 Hz, H^3, H^5-piperazine), 2.67 (t, 2H, J = 7.0 Hz, -*N*-C$\underline{H}_2$-CH_2-), 2.55 (t, 4H, J = 4.8 Hz, H^2, H^6-piperazine), 2.51–2.47 (m, 2H, -*N*–CH_2–C$\underline{H}_2$-, with DMSO). ^{13}C NMR (DMSO-d_6) δ: 170.0, 168.4, 155.9 (d, J = 234.7 Hz), 147.8 (d, J = 2.3 Hz), 134.9, 133.2, 121.5, 117.9, 117.0 (d, J = 7.6 Hz), 115.1 (d, J = 22.1 Hz), 113.3, 111.2, 53.6, 52.4, 48.9, 34.0, 28.9. HRMS (ESI) [M+H]$^+$ *m/z* for $C_{21}H_{24}FN_4O_2S$ calculated: 415.1604, found: 415.1608. Anal. Calcd. for $C_{21}H_{23}FN_4O_2S$: C, 60.85; H, 5.59; N, 13.52; S, 7.74. Found: C, 60.46; H, 5.90; N, 13.17; S, 7.60.

4.1.7.3. 3-[4-(4-Chlorophenyl)piperazin-1-yl]-N-(3-methyl-2-oxo-2,3-dihydrobenzothiazol-6-yl)propanamide ***(9c)***. Compound **9c** was obtained by using method B from intermediate **6** (360 mg, 2 mmol), 3-[4-(4-chlorophenyl)piperazin-1-yl]propanoic acid (591 mg, 2.2 mmol), EDC (460 mg, 2.4 mmol) and DMAP (49 mg, 0.4 mmol). Then it was recrystallized from butanol. Yield: 620 mg, 72%; mp: 200.3 C. ^{1}H NMR (DMSO-d_6) δ: 10.11 (s, 1H, *N*–H), 7.93 (d, 1H, J = 2.0 Hz, H^7), 7.48 (dd, 1H, J = 8.7 Hz, J = 2 0.0 Hz, H^5), 7.23 (d, 1H, J = 8.7 Hz, H^4), 7.21 (d, 2H, J = 8.4 Hz, H$^{3'}$, H$^{5'}$), 6.94 (d, 2H, J = 8.4 Hz, H$^{2'}$, H$^{6'}$), 3.37 (s, 3H, *N*–CH_3), 3.22–3.10 (m, 6H, H^3, H^5-piperazine, -*N*-C$\underline{H}_2$-CH_2-), 2.66–2.50 (m, 6H, H^2,H^6-piperazine, -*N*–CH_2–C$\underline{H}_2$-). ^{13}C NMR (DMSO-d_6) δ: 169.5, 168.3, 149.4, 134.9, 133.2, 128.5, 122.5, 121.4, 118.0, 116.8, 113.3, 111.2, 53.1, 51.9, 47.4, 33.3, 28.9. HRMS (ESI) [M+H]$^+$ *m/z* for $C_{21}H_{24}ClN_4O_2S$ calculated: 431.1309, found: 431.1317. Anal. Calcd. for $C_{21}H_{23}ClN_4O_2S \cdot 1H_2O$: C, 56.18; H, 5.61; N, 12.48; S, 7.14. Found: C, 56.14; H, 5.75; N, 12.38; S, 7.09.

4.1.7.4. 3-[4-(4-Methylphenyl)piperazin-1-yl]-N-(3-methyl-2-oxo-2,3-dihydrobenzothiazol-6-yl)propanamide ***(9d)***. Compound **9d** was obtained by using method B from intermediate **6** (360 mg, 2 mmol), 3-[4-(4-methylphenyl)piperazin-1-yl]propanoic acid (546 mg, 2.2 mmol), EDC (460 mg, 2.4 mmol) and DMAP (49 mg, 0.4 mmol). Then it was recrystallized from butanol. Yield: 738 mg, 90%; mp: 216.8 C. ^{1}H NMR (DMSO-d_6) δ: 10.15 (s, 1H, *N*–H), 7.95 (d, 1H, J = 2.0 Hz, H^7), 7.46 (dd, 1H, J = 8.8 Hz, J = 2 Hz, H^5), 7.22 (d, 1H, J = 8.8 Hz, H^4), 6.99 (d, 2H, J = 8.4 Hz, H$^{3'}$, H$^{5'}$), 6.80 (d, 2H, J = 8.4 Hz, H$^{2'}$, H$^{6'}$), 3.35 (s, 3H, *N*–CH_3), 3.05 (t, 4H, J = 4.7 Hz, H^3, H^5-piperazine), 2.67 (t, 2H, J = 7.0 Hz, -*N*-C$\underline{H}_2$-CH_2-), 2.55 (t, 4H, J = 4.7 Hz, H^2, H^6 piperazine), 2.52–2.47 (m, 2H, -*N*–CH_2–C$\underline{H}_2$-, with DMSO), 2.18 (s, 3H, phenyl-CH_3). ^{13}C NMR (DMSO-d_6) δ ppm: 170.0, 168.4, 148.9, 135.0, 133.2, 129.3, 127.5, 121.5, 117.9, 115.6, 113.3, 111.3, 53.7, 52.4, 48.6, 34.0, 28.9, 20.0. HRMS (ESI) [M+H]$^+$ *m/z* for $C_{22}H_{27}N_4O_2S$ calculated: 411.1855, found: 411.1861. Anal. Calcd. for $C_{22}H_{26}N_4O_2S$: C, 64.36; H, 6.38; N, 13.65; S, 7.81. Found: C, 64.27; H, 6.44; N, 13.55; S, 7.76.

4.1.7.5. 3-[4-(4-Methoxyphenyl)piperazin-1-yl]-N-(3-methyl-2-oxo-2,3-dihydrobenzothiazol-6-yl)propanamide ***(9e)***. Compound **9e** was obtained by using method B from intermediate **6** (360 mg, 2 mmol), 3-[4-(4-methoxyphenyl)piperazin-1-yl]propanoic acid (582 mg, 2.2 mmol), EDC (460 mg, 2.4 mmol) and DMAP (49 mg, 0.4 mmol). Then it was recrystallized from butanol. Yield: 734 mg, 86%; mp: 192.6 C. ^{1}H NMR (DMSO-d_6) δ: 10.17 (s, 1H, *N*–H), 7.96 (d, 1H, J = 2.0 Hz, H^7), 7.46 (dd, 1H, J = 8.9 Hz, J = 2 Hz, H^5), 7.23 (d, 1H, J = 8.9 Hz, H^4), 6.87 (d, 2H, J = 8.8 Hz, H$^{3'}$, H$^{5'}$), 6.79 (d, 2H, J = 8.8 Hz, H$^{2'}$, H$^{6'}$), 3.67 (s, 3H, *O*–CH_3), 3.36 (s, 3H, *N*–CH_3), 3.00 (t, 4H, J = 4.8 Hz, H^3,H^5-piperazine), 2.68 (t, 2H, J = 7.0 Hz, -*N*-C$\underline{H}_2$-CH_2-), 2.56 (t, 4H, J = 4.8 Hz, H^2,H^6-piperazine), 2.51–2.48 (m, 2H, -*N*–CH_2–C$\underline{H}_2$-, with DMSO). ^{13}C NMR (DMSO-d_6) δ: 170.0, 168.4, 152.8, 145.3, 135.0, 133.2, 121.5, 117.9, 117.2, 114.2, 113.3, 111.3, 55.1, 53.7, 52.5, 49.5, 34.0, 28.9. HRMS (ESI) [M+H]$^+$ *m/z* for $C_{22}H_{27}N_4O_3S$ calculated: 427.1804, found: 427.1802. Anal. Calcd. for $C_{22}H_{26}N_4O_3S$: C, 61.95; H, 6.14; N, 13.14; S, 7.52. Found: C, 62.17; H, 6.20; N, 13.09; S, 7.52.

4.1.7.6. 3-[4-(4-Trifluoromethylphenyl)piperazin-1-yl]-N-(3-methyl-2-oxo-2,3-dihydrobenzothiazol-6-yl)propanamide ***(9f)***. Compound **9f** was obtained by using method B from intermediate **6** (360 mg, 2 mmol), 3-[4-(4-trifluoromethylphenyl)piperazin-1-yl] propanoic acid (665 mg, 2.2 mmol), EDC (460 mg, 2.4 mmol) and DMAP (49 mg, 0.4 mmol). Then it was recrystallized from ethanol. Yield: 743 mg, 80%; mp: 213.6 C. ^{1}H NMR (DMSO-d_6) δ: 10.11 (s, 1H, *N*–H), 7.95 (d, 1H, J = 1.6 Hz, H^7), 7.50–7.47 (m, 3H, H$^{3'}$, H$^{5'}$, H^5), 7.23 (d, 1H, J = 8.4 Hz, H^4), 7.05 (d, 2H, J = 8.4 Hz, H$^{2'}$, H$^{6'}$), 3.37 (s, 3H, *N*–CH_3), 3.28 (t, 4H, J = 4.5 Hz, H^3, H^5-piperazine), 2.70 (t, 2H, J = 6.8 Hz, -*N*-C$\underline{H}_2$-CH_2-), 2.57 (t, 4H, J = 4.5 Hz, H^2, H^6-piperazine), 2.54–2.49 (m, 2H, -*N*–CH_2–C$\underline{H}_2$-, with DMSO). ^{13}C NMR (DMSO-d_6) δ: 169.9, 168.3, 153.1, 134.9, 133.2, 126.0 (q, J = 3.8 Hz), 124.9 (q, J = 269.0 Hz), 121.4, 117.9, 117.7 (q, J = 35.5 Hz), 114.0, 113.3, 111.1, 53.5, 52.0, 46.9, 34.0, 28.8. HRMS (ESI) [M+H]$^+$ *m/z* for $C_{22}H_{24}F_3N_4O_2S$ calculated: 465.1572, found: 465.1574. Anal. Calcd. for $C_{22}H_{23}F_3N_4O_2S$: C, 56.89; H, 4.99; N, 12.06; S, 6.90. Found: C, 56.97; H, 4.86; N, 12.11; S, 6.91.

4.1.7.7. 3-(4-Benzylpiperazin-1-yl)-N-(3-methyl-2-oxo-2,3-dihydrobenzothiazol-6-yl)propanamide ***(9g)***. Compound **9g** was obtained by using method B from intermediate **6** (360 mg, 2 mmol), 3-(4-benzylpiperazin-1-yl)propanoic acid (546 mg, 2.2 mmol), EDC (460 mg, 2.4 mmol) and DMAP (49 mg, 0.4 mmol). Then it was recrystallized from 2-propanol. Yield: 575 mg, 70%; mp: 183.3 C. ^{1}H NMR (DMSO-d_6) δ: 10.15 (s, 1H, *N*–H), 7.94 (d, 1H, J = 2.0 Hz, H^7), 7.44 (dd, 1H, J = 8.6 Hz, J = 2.0 Hz, H^5), 7.33–7.22 (m, 6H, H^4, phenyl protons), 3.44 (s, 2H, –CH_2- C_6H_5), 3.37 (s, 3H, *N*–CH_3), 2.61 (t, 2H, J = 6.9 Hz, -*N*-C$\underline{H}_2$-CH_2-), 2.45 (t, 2H, J = 6.9 Hz, -*N*–CH_2–C$\underline{H}_2$-), 2.40–2.32 (m, 8H, piperazine). ^{13}C NMR (DMSO-d_6) δ: 170.0, 168.4, 138.1, 134.9, 133.2, 128.7, 128.1, 126.8, 121.4, 117.8, 113.3, 111.3, 62.0, 53.7, 52.6, 52.4, 34.0, 28.9. HRMS (ESI) [M+H]$^+$ *m/z* for $C_{22}H_{27}N_4O_2S$ calculated: 411.1855, found: 411.1847. Anal. Calcd. for $C_{22}H_{26}N_4O_2S$: C, 64.36; H, 6.38; N, 13.65; S, 7.81. Found: C, 64.39; H, 6.37; N, 13.58; S, 7.79.

4.1.7.8. 3-[4-(4-Fluorobenzyl)piperazin-1-yl]-N-(3-methyl-2-oxo-2,3-dihydrobenzothiazol-6-yl)propanamide ***(9h)***. Compound **9h** was obtained by using method B from intermediate **6** (360 mg, 2 mmol), 3-[4-(4-fluorobenzyl)piperazin-1-yl]propanoic acid (585 mg, 2.2 mmol), EDC (460 mg, 2.4 mmol) and DMAP (49 mg, 0.4 mmol). Then it was recrystallized from 2-propanol. Yield: 608 mg, 71%; mp: 176.7 C. ^{1}H NMR (DMSO-d_6) δ: 10.15 (s, 1H, *N*–H), 7.94 (d, 1H, J = 2.0 Hz, H^7), 7.44 (dd, 1H, J = 8.8 Hz, J = 2.0 Hz, H^5), 7.32–7.28 (m, 2H, H$^{2'}$, H$^{6'}$), 7.23 (d, 1H, J = 8.8 Hz, H^4), 7.14–7.10 (m, 2H, H$^{3'}$, H$^{5'}$), 3.42 (s, 2H, –CH_2-C_6H_5), 3.37 (s, 3H, *N*–CH_3), 2.61 (t, 2H, J = 7.0 Hz, -*N*-C$\underline{H}_2$-CH_2-), 2.45 (t, 2H, J = 7.0 Hz, -*N*–CH_2–C$\underline{H}_2$-), 2.40–2.30 (m, 8H, piperazine). ^{13}C NMR (DMSO-d_6) δ: 170.0, 168.4, 161.1 (d, J = 240.8 Hz), 134.3, 134.3, 133.2, 130.5 (d, J = 7.6 Hz), 121.4, 117.8, 114.8 (d, J = 21.3 Hz), 113.3, 111.2, 61.0, 53.5, 52.5, 52.4, 34.0, 28.9. HRMS (ESI) [M+H]$^+$ *m/z* for $C_{22}H_{26}FN_4O_2S$ calculated: 429.1761, found: 429.1754. Anal. Calcd. for $C_{22}H_{25}FN_4O_2S$: C, 61.66; H, 5.88; N, 13.07; S, 7.48. Found: C, 61.27; H, 5.81; N, 12.93; S, 7.48.

4.1.7.9. 3-[4-(4-Chlorobenzyl)piperazin-1-yl]-N-(3-methyl-2-oxo-2,3-dihydrobenzothiazol-6-yl)propanamide ***(9i)***. Compound **9i** was obtained by using method B from intermediate **6** (360 mg, 2 mmol), 3-[4-(4-chlorobenzyl)piperazin-1-yl]propanoic acid (622 mg, 2.2 mmol), EDC (460 mg, 2.4 mmol) and DMAP (49 mg, 0.4 mmol). Then it was recrystallized from ethanol. Yield: 783 mg, 88%; mp:

184.9 C. ^{1}H NMR (DMSO-d_6) δ: 10.11 (s, 1H, *N*–H), 7.93 (d, 1H, J = 2.1 Hz, H^7), 7.44 (dd, 1H, J = 8.5 Hz, J = 2.1 Hz, H^5), 7.35 (d, 2H, J = 8.2 Hz, $H^{2'}$, $H^{6'}$), 7.29 (d, 2H, J = 8.2 Hz, $H^{3'}$, $H^{5'}$),7.22 (d, 1H, J = 8.5 Hz, H^4), 3.43 (s, 2H, $-CH_2$-C_6H_5), 3.36 (s, 3H, *N*–CH_3), 2.62 (t, 2H, J = 7.0 Hz, -*N*-C<u>H</u>$_2$-CH_2-), 2.46 (t, 2H, J = 7.0 Hz, -*N*–CH_2–C<u>H</u>$_2$-), 2.42–2.32 (m, 8H, piperazine). ^{13}C NMR (DMSO-d_6) δ: 169.6, 168.3, 137.2, 134.9, 133.1, 131.3, 130.4, 128.0, 121.4, 117.8, 113.2, 111.1, 60.9, 53.6, 52.4, 52.3, 33.9, 28.8. HRMS (ESI) $[M+H]^+$ *m*/*z* for $C_{22}H_{26}ClN_4O_2S$ calculated: 445.1465, found: 445.1465. Anal. Calcd. for $C_{22}H_{25}ClN_4O_2S$: C, 59.38; H, 5.66; N, 12.59; S, 7.21. Found: C, 59.43; H, 5.87; N, 12.69; S, 7.31.

4.1.7.10. 3-[4-(4-Methoxybenzyl)piperazin-1-yl]-N-(3-methyl-2-oxo-2,3-dihydrobenzothiazol-6-yl)propanamide ***(9j)***. Compound **9j** was obtained by using method B from intermediate **6** (360 mg, 2 mmol), 3-[4-(4-methoxybenzyl)piperazin-1-yl]propanoic acid (612 mg, 2.2 mmol), EDC (460 mg, 2.4 mmol) and DMAP (49 mg, 0.4 mmol). Then it was recrystallized from 2-propanol. Yield: 608 mg, 69%; mp: 175.2 C. ^{1}H NMR (DMSO-d_6) δ: 10.12 (s, 1H, *N*–H), 7.93 (d, 1H, J = 2.0 Hz, H^7), 7.43 (dd, 1H, J = 8.4 Hz, J = 2.0 Hz, H^5), 7.22 (d, 1H, J = 8.4 Hz, H^4), 7.17 (d, 2H, J = 8.2 Hz, $H^{2'}$, $H^{6'}$), 6.86 (d, 2H, J = 8.2 Hz, $H^{3'}$, $H^{5'}$), 3.72 (s, 3H, *O*–CH_3), 3.36 (s, 5H, $-CH_2$-C_6H_5, *N*–CH_3), 2.61 (t, 2H, J = 7.0 Hz, -*N*-C<u>H</u>$_2$-CH_2-), 2.44 (t, 2H, J = 7.0. Hz, -*N*–CH_2–C<u>H</u>$_2$-), 2.38–2.30 (m, 8H, piperazine). ^{13}C NMR (DMSO-d_6) δ: 169.9, 168.3, 158.1, 134.9, 133.1, 129.9, 129.8, 121.4, 117.8, 113.4, 113.2, 111.1, 61.3, 54.8, 53.6, 52.4, 52.3, 33.9, 28.8. HRMS (ESI) $[M+H]^+$ *m*/*z* for $C_{23}H_{29}N_4O_3S$ calculated: 441.1960, found: 441.1958. Anal. Calcd. for $C_{23}H_{28}N_4O_3S$: C, 62.70; H, 6.41; N, 12.72; S, 7.28. Found: C, 62.59; H, 6.59; N, 12.69; S, 7.32.

4.1.7.11. 3-[4-(4-Trifluoromethylbenzyl)piperazin-1-yl]-N-(3-methyl-2-oxo-2,3-dihydrobenzothiazol-6-yl)propanamide ***(9k)***. Compound **9k** was obtained by using method B from intermediate **6** (360 mg, 2 mmol), 3-[4-(4-trifluoromethylbenzyl)piperazin-1-yl] propanoic acid (696 mg, 2.2 mmol), EDC (460 mg, 2.4 mmol) and DMAP (49 mg, 0.4 mmol). Then it was recrystallized from butanol. Yield: 574 mg, 60%; mp: 190.8 C. ^{1}H NMR (DMSO-d_6) δ: 10.11 (s, 1H, *N*–H), 7.93 (d, 1H, J = 2.0 Hz, H^7), 7.66 (d, 2H, J = 8.2 Hz, $H^{3'}$, $H^{5'}$), 7.51 (d, 2H, J = 8.2 Hz, $H^{2'}$, $H^{6'}$), 7.44 (dd, 1H, J = 8.5 Hz, J = 2.0 Hz, H^5), 7.22 (d, 1H, J = 8.5 Hz, H^4), 3.54 (s, 2H, $-CH_2$-C_6H_5), 3.36 (s, 3H, *N*–CH_3), 2.62 (t, 2H, J = 7.0 Hz, -*N*-C<u>H</u>$_2$-CH_2-), 2.47 (t, 2H, J = 7.0 Hz, -*N*–CH_2–C<u>H</u>$_2$-), 2.42–2.37 (m, 8H, piperazine). ^{13}C NMR (DMSO-d_6) δ: 169.9, 168.3, 143.3, 134.9, 133.1, 129.2, 127.5 (q, J = 31.5 Hz), 124.9 (q, J = 3.8 Hz), 124.2 (q, J = 269.7 Hz), 121.4, 117.8, 113.2, 111.2, 61.2, 53.6, 52.5, 52.3, 34.0, 28.8. HRMS (ESI) $[M+H]^+$ *m*/*z* for $C_{23}H_{26}F_3N_4O_2S$ calculated: 479.1729, found: 479.1727. Anal. Calcd. for $C_{23}H_{25}F_3N_4O_2S$: C, 57.73; H, 5.27; N, 11.71; S, 6.70. Found: C, 57.78; H, 5.48; N, 11.62; S, 6.74.

4.1.7.12. 3-(4-Phenylpiperidin-1-yl)-N-(3-methyl-2-oxo-2,3-dihydrobenzoxazol-6-yl)propanamide ***(9l)***. Compound **9l** was obtained following method B using intermediate **6** (360 mg, 2 mmol), 3-(4-phenylpiperidin-1-yl)propanoic acid (513 mg, 2.2 mmol), EDC (460 mg, 2.4 mmol) and DMAP (49 mg, 0.4 mmol). Then it was recrystallized from ethanol. Yield: 577 mg, 73%; mp: 185.1 C. ^{1}H NMR (DMSO-d_6) δ: 10.19 (s, 1H, *N*–H), 7.98 (d, 1H, J = 2.0 Hz, H^7), 7.47 (dd, 1H, J = 8.8 Hz, J = 2.0 Hz, H^5), 7.30–7.15 (m, 6H, H^4, phenyl protons), 3.37 (s, 3H, *N*–CH_3), 3.00 (d, 2H, J = 11.6 Hz, H^{2e}, H^{6e}-piperidine), 2.67 (t, 2H, J = 7.0 Hz, -*N*-C<u>H</u>$_2$-CH_2-), 2.51–2.44 (m, 3H, H^4-piperidine, -*N*–CH_2–C<u>H</u>$_2$-, with DMSO), 2.06 (td, 2H, J = 11.6 Hz, J = 2.0. Hz, H^{2a}, H^{6a}-piperidine), 1.76–1.59 (m, 4H, H^3, H^5-piperidine). ^{13}C NMR (DMSO-d_6) δ: 170.2, 168.4, 146.1, 135.0, 135.2, 128.2, 126.6, 125.9, 121.5, 117.9, 113.3, 111.3, 54.0, 53.4, 41.7, 34.2, 33.0, 28.9. HRMS (ESI) $[M+H]^+$ *m*/*z* for $C_{22}H_{26}N_3O_2S$ calculated: 396.1746, found: 396.1739. Anal. Calcd. for $C_{22}H_{25}N_3O_2S$: C, 66.81; H, 6.37; N, 10.62; S, 8.11. Found: C, 66.83; H, 6.43; N, 10.65; S, 8.12.

4.1.7.13. 3-(4-Benzylpiperidin-1-yl)-N-(3-methyl-2-oxo-2,3-dihydrobenzoxazol-6-yl)propanamide ***(9m)***. Compound **9m** was obtained following method B using intermediate **6** (360 mg, 2 mmol), 3-(4-benzylpiperidin-1-yl)propanoic acid (544 mg, 2.2 mmol), EDC (460 mg, 2.4 mmol) and DMAP (49 mg, 0.4 mmol). Then it was recrystallized from 2-propanol. Yield: 606 mg, 74%; mp: 156.4 C. ^{1}H NMR (DMSO-d_6) δ: 10.19 (s, 1H, *N*–H), 7.96 (d, 1H, J = 2.3 Hz, H^7), 7.43 (dd, 1H, J = 9.0 Hz, J = 2.3 Hz, H^5), 7.28–7.13 (m, 6H, H^4, phenyl protons), 3.37 (s, 3H, *N*–CH_3), 2.85 (d, 2H, J = 10.9 Hz, H^{2e}, H^{6e}-piperidin), 2.58 (t, 2H, J = 6.9 Hz, -*N*-C<u>H</u>$_2$-CH_2-), 2.52–2.46 (m, 2H, $-CH_2$-C_6H_5, with DMSO), 2.43 (t, 2H, J = 6.9 Hz, -*N*–CH_2–C<u>H</u>$_2$-), 1.87 (t, 2H, J = 10.9 Hz, H^{2a}, H^{6a}-piperidine), 1.55–1.42 (m, 3H, H^{3e}, H^{5e}, H^4-piperidine), 1.21–1.10 (m, 2H, H^{3a}, H^{5a}-piperidine). ^{13}C NMR (DMSO-d_6) δ: 170.1, 168.4, 140.3, 135.0, 133.2, 128.9, 128.0, 125.7, 121.5, 117.8, 113.2, 111.3, 54.0, 52.9, 42.3, 37.3, 34.1, 31.7, 28.9. HRMS (ESI) $[M+H]^+$ *m*/*z* for $C_{23}H_{28}N_3O_2S$ calculated: 410.1902, found: 410.1902. Anal. Calcd. for $C_{23}H_{27}N_3O_2S$: C, 67.45; H, 6.65; N, 10.26; S, 7.83. Found: C, 67.83; H, 6.68; N, 10.31; S, 7.83.

4.1.7.14. 3-[Benzyl(methyl)amino]-N-(3-methyl-2-oxo-2,3-dihydrobenzoxazol-6-yl)propanamide ***(9n)***. Compound **9n** was obtained following method B using intermediate **6** (360 mg, 2 mmol), 3-[benzyl(methyl)amino]propanoic acid (425 mg, 2.2 mmol), EDC (460 mg, 2.4 mmol) and DMAP (49 mg, 0.4 mmol). Then it was recrystallized from ethanol. Yield: 270 mg, 38%; mp: 119.9 C. ^{1}H NMR (DMSO-d_6) δ: 10.07 (s, 1H, *N*–H), 7.94 (d, 1H, J = 2.0 Hz, H^7), 7.46 (dd, 1H, J = 8.7 Hz, J = 2.0 Hz, H^5), 7.30–7.25 (m, 5H, phenyl protons), 7.23 (d, 1H, J = 8.7 Hz, H^4), 3.50 (s, 2H, $-CH_2$-C_6H_5), 3.37 (s, 3H, *N*–CH_3), 2.69 (t, 2H, J = 7.0 Hz, -*N*-C<u>H</u>$_2$-CH_2-), 2.54–2.48 (m, 2H, -*N*–CH_2–C<u>H</u>$_2$-, with DMSO), 2.15 (s, 3H, N_2–CH_3). ^{13}C NMR (DMSO-d_6) δ: 170.0, 168.3, 138.8, 134.9, 133.1, 128.5, 127.9, 126.7, 121.4, 117.9, 113.3, 111.1, 61.0, 52.9, 41.5, 34.5, 28.8. HRMS (ESI) $[M+H]^+$ *m*/*z* for $C_{19}H_{22}N_3O_2S$ calculated: 356.1433, found: 356.1435. Anal. Calcd. for $C_{19}H_{21}N_3O_2S$: C, 64.20; H, 5.95; N, 11.82; S, 9.02. Found: C, 63.92; H, 6.14; N, 11.75; S, 8.98.

4.1.8. General procedure for the preparation of 4-substitutedbutanoic acid intermediates

The appropriate amine derivative (1 equivalent), ethyl 4-bromobutyrate (1 equivalent) and potassium carbonate (1.5 equivalent) were dissolved in 20 ml ACN and stirred under reflux condition for 6 h. The end of this period, potassium carbonate was filtered and ACN was evaporated to dryness. The remaining residue (corresponding ester derivatives) was hydrolyzed with 5% NaOH solution by heating at 40 C for 2 h and obtained the sodium salt of the corresponding butanoic acid derivatives. Then, the reaction mixture was cooled down and neutralized with HCl solution. To obtain the carboxylic acid derivatives, water was evaporated under reduced pressure and the mixture was separated from sodium chloride with the aid of acetone. The resulting oil gained by evaporating acetone was solidified with ether and used in the synthesis of the butanamide derivatives.

4.1.9. General procedure for the preparation of 4-substitutedbutanamide derivatives bearing benzoxazolone or benzothiazolone ***(10a-c)***

4-Substituted-*N*-(3-methyl-2-oxo-2,3-dihydro-1,3-benzoxazol-6-yl)butanamide derivative **(10a)** and 4-substituted-*N*-(3-methyl-2-oxo-2,3-dihydro-1,3-benzothiazol-6-yl)butanamide derivatives (**10b** and **10c**) were synthesized by following method B as

mentioned in section 4.1.7 from intermediate **5** or **6** (1 equivalent), the corresponding butanoic acid (1.1 equivalent), EDC (1.2 equivalent) and DMAP (0.2 equivalent).

*4.1.9.1. 4-(4-Benzylpiperazin-1-yl)-N-(3-methyl-2-oxo-2,3-dihydrobenzoxazol-6-yl)butanamide **(10a)**.* Compound **10a** was obtained by using method B from intermediate **5** (350 mg, 2 mmol), 4-(4-benzylpiperazin-1-yl)butanoic acid (616 mg, 2.2 mmol), EDC (491 mg, 2.4 mmol) and DMAP (52 mg, 0.4 mmol). Then it was recrystallized from ACN. Yield: 153 mg, 18%; mp: 190.3 C. ^{1}H NMR (DMSO-d_6) δ: 9.94 (s, 1H, *N*–H), 7.73 (d, 1H, J = 1.6 Hz, H^7), 7.30–7.20 (m, 6H, phenyl protons, H^5), 7.15 (d, 1H, J = 1.6 Hz, H^4), 3.41 (s, 2H, –CH$_2$-C$_6$H$_5$), 3.30 (s, 3H, *N*–CH$_3$), 2.40–2.24 (m, 12H, H-piperazine, -CH$_2$-CH$_2$-CH$_2$-), 1.72 (p, 2H, J = 7.2 Hz, -CH$_2$-CH$_2$-CH$_2$-). ^{13}C NMR (DMSO-d_6) δ: 171.0, 154.1, 141.7, 138.2, 134.5, 128.7, 128.0, 127.0, 126.8, 114.4, 108.7, 101.4, 62.0, 57.2, 52.7, 52.6, 34.3, 28.0, 22.1. HRMS (ESI) [M+H]$^+$ *m/z* for $C_{23}H_{29}N_4O_3$ calculated: 409.2240, found: 409.2246. Anal. Calcd. for $C_{23}H_{28}N_4O_3$: C, 67.63; H, 6.91; N, 13.72. Found: C, 67.29; H, 7.29; N, 11.75; S, 13.64.

*4.1.9.2. 4-(4-Benzylpiperazin-1-yl)-N-(3-methyl-2-oxo-2,3-dihydrobenzothiazol-6-yl)butanamide **(10b)**.* Compound **10b** was obtained by using method B from intermediate **6** (400 mg, 2.2 mmol), 4-(4-benzylpiperazin-1-yl)butanoic acid (641 mg, 2.42 mmol), EDC (512 mg, 2.64 mmol) and DMAP (54 mg, 0.44 mmol). Then it was recrystallized from butanol. Yield: 150 mg, 16%; mp: 87.3 C. ^{1}H NMR (DMSO-d_6) δ: 9.92 (s, 1H, *N*–H), 7.94 (d, 1H, J = 2.0 Hz, H^7), 7.41 (dd, 1H, J = 8.8 Hz, J = 2.0 Hz, H^5), 7.30–7.18 (m, 6H, phenyl protons, H^4), 3.39 (s, 2H, –CH$_2$-C$_6$H$_5$), 3.31 (s, 3H, *N*–CH$_3$), 2.38–2.24 (m, 12H, H-piperazine, -CH$_2$-CH$_2$-CH$_2$-), 1.69 (p, 2H, J = 7.2 Hz, –CH$_2$-CH$_2$-CH$_2$-). ^{13}C NMR (DMSO-d_6) δ: 170.1, 168.2, 138.1, 135.0, 133.0, 128.6, 128.0, 126.7, 121.3, 117.8, 113.2, 111.1, 62.0, 57.1, 52.6, 52.5, 34.2, 28.8, 22.1. HRMS (ESI) [M+H]$^+$ *m/z* for $C_{23}H_{29}N_4O_2S$ calculated: 425.2011, found: 425.2015. Anal. Calcd. for $C_{23}H_{28}N_4O_2S\cdot 3H_2O$: C, 57.72; H, 7.16; N, 11.71; S, 6.81. Found: C, 57.49; H, 7.00; N, 11.80; S, 6.70.

*4.1.9.3. 4-(4-Phenylpiperidin-1-yl)-N-(3-methyl-2-oxo-2,3-dihydrobenzothiazol-6-yl)butanamide **(10c)**.* Compound **10c** was obtained by using method B from intermediate **6** (500 mg, 2.8 mmol), 4-(4-phenylpiperidin-1-yl)butanoic acid (756 mg, 3.1 mmol), EDC (639 mg, 3.4 mmol) and DMAP (68 mg, 0.6 mmol). Then it was recrystallized from 2-propanol. Yield: 600 mg, 53%; mp: 104.6 C. ^{1}H NMR (DMSO-d_6) δ: 9.95 (s, 1H, *N*–H), 7.99 (d, 1H, J = 2.0 Hz, H^7), 7.48 (dd, 1H, J = 8.6 Hz, J = 2.0 Hz, H^5), 7.23–7.07 (m, 6H, phenyl protons, H^4), 3.35 (s, 3H, *N*–CH$_3$), 2.91 (d, 2H, J = 11.4 Hz, H^{2e}, H^{6e}-piperidine), 2.44–2.28 (m, 5H, H^4-piperidine, -*N*-CH$_2$-CH$_2$-CH$_2$-), 1.91 (td, 2H, J = 11.4 Hz, J = 1.8 Hz, H^{2a}, H^{6a}-piperidin), 1.76 (p, 2H, J = 6.8 Hz, -*N*–CH$_2$–CH$_2$-CH$_2$-) 1.68–1.48 (m, 4H, H^3, H^5-piperidine). ^{13}C NMR (DMSO-d_6) δ: 171.2, 168.4, 146.3, 135.4, 133.0, 128.1, 126.6, 125.9, 121.4, 117.8, 113.1, 111.2, 57.7, 53.7, 41.9, 34.7, 33.1, 28.9, 22.4. HRMS (ESI) [M+H]$^+$ *m/z* for $C_{23}H_{28}N_3O_2S$ calculated: 410.1902, found: 410.1899. Anal. Calcd. for $C_{23}H_{27}N_4O_2S\cdot 3H_2O$: C, 63.94; H, 6.88; N, 9.73; S, 7.42. Found: C, 63.96; H, 7.07; N, 9.88; S, 7.51.

4.1.10. General procedure for the preparation of 5-substitutedpentanoic acid intermediates

5-Substitutedpentanoic acid intermediates were produced by following the procedure in section 4.1.8 from appropriate amin derivatives (1 equivalent), ethyl 5-bromovalerate (1 equivalent) and potassium carbonate (1.5 equivalent).

*4.1.11. General procedure for the preparation of 5-substitutedpentanamide derivatives bearing benzoxazolone or benzothiazolone **(11a-c)***

5-Substituted-*N*-(3-methyl-2-oxo-2,3-dihydro-1,3-benzoxazol-6-yl)pentanmide derivative **(11a)** and 5-substituted-*N*-(3-methyl-2-oxo-2,3-dihydro-1,3-benzothiazol-6-yl)pentanmide derivatives **(11b** and **11c)** were synthesized by following method B as mentioned in section 4.1.7 from intermediate **5** or **6** (1 equivalent), the corresponding pentanoic acid (1.1 equivalent), EDC (1.2 equivalent) and DMAP (0.2 equivalent).

*4.1.11.1. 5-(4-Benzylpiperazin-1-yl)-N-(3-methyl-2-oxo-2,3-dihydrobenzoxazol-6-yl)pentanamide **(11a)**.* Compound **11a** was obtained by using method B from intermediate **5** (600 mg, 3.6 mmol), 5-(4-benzylpiperazin-1-yl)pentanoic acid (1110 mg, 4 mmol), EDC (841 mg, 4.4 mmol) and DMAP (89 mg, 0.7 mmol). Then it was recrystallized from acetone-hexane. Yield: 347 mg, 22%; mp: 138.4 C. ^{1}H NMR (DMSO-d_6) δ: 9.92 (s, 1H, *N*–H), 7.70 (d, 1H, J = 1.6 Hz, H^7), 7.30–7.17 (m, 6H, phenyl protons, H^5), 7.12 (d, 1H, J = 8.8 Hz, H^4), 3.40 (s, 2H, –CH$_2$-C$_6$H$_5$), 3.28 (s, 3H, *N*–CH$_3$), 2.36–2.21 (m, 12H, H-piperazine, *N*–CH$_2$–CH$_2$–CH$_2$–CH$_2$-), 1.56 (p, 2H, J = 7.5 Hz, *N*–CH$_2$–CH$_2$–CH$_2$–CH$_2$-), 1.41 (p, 2H, J = 7.5 Hz, *N*–CH$_2$–CH$_2$–CH$_2$–CH$_2$-). ^{13}C NMR (DMSO-d_6) δ: 171.0, 154.1, 141.7, 138.2, 134.5, 128.7, 128.0, 127.0, 126.8, 114.4, 108.7, 101.4, 62.1, 57.5, 52.7, 52.6, 36.1, 27.9, 25.9, 23.0. HRMS (ESI) [M+H]$^+$ *m/z* for $C_{24}H_{31}N_4O_3$ calculated: 423.2396, found: 423.2387. Anal. Calcd. for $C_{24}H_{30}N_4O_3$: C, 68.22; H, 7.16; N, 13.26. Found: C, 67.97; H, 7.45; N, 9.88.

*4.1.11.2. 5-(4-Benzylpiperazin-1-yl)-N-(3-methyl-2-oxo-2,3-dihydrobenzothiazol-6-yl)pentanamide **(11b)**.* Compound **11b** was obtained by using method B from intermediate **6** (600 mg, 3.3 mmol), 5-(4-benzylpiperazin-1-yl)pentanoic acid (1012 mg, 3.6 mmol), EDC (767 mg, 4 mmol) and DMAP (81 mg, 0.7 mmol). Then it was recrystallized from acetone-hexane. Yield: 420 mg, 41%; mp: 120.8 C. ^{1}H NMR (DMSO-d_6) δ: 9.96 (s, 1H, *N*–H), 7.97 (d, 1H, J = 2.0 Hz, H^7), 7.47 (dd, 1H, J = 9.0 Hz, J = 2.0 Hz, H^5), 7.31–7.21 (m, 6H, phenyl protons, H^4), 3.43 (s, 2H, –CH$_2$-C$_6$H$_5$), 3.36 (s, 3H, *N*–CH$_3$), 2.40–2.24 (m, 12H, H-piperazine, *N*–CH$_2$–CH$_2$–CH$_2$–CH$_2$-), 1.59 (p, 2H, J = 7.4 Hz, *N*–CH$_2$–CH$_2$–CH$_2$–CH$_2$-), 1.44 (p, 2H, J = 7.4 Hz, *N*–CH$_2$–CH$_2$–CH$_2$–CH$_2$-). ^{13}C NMR (DMSO-d_6) δ: 171.0, 168.3, 138.2, 135.1, 133.1, 128.7, 128.0, 126.8, 121.4, 117.9, 113.3, 111.2, 62.0, 57.5, 52.7, 52.6, 36.1, 28.9, 25.8, 23.0. HRMS (ESI) [M+H]$^+$ *m/z* for $C_{24}H_{31}N_4O_2S$ calculated: 439.2168, found: 439.2188. Anal. Calcd. for $C_{24}H_{30}N_4O_2S.2,5H_2O$: C, 59.60; H, 7.29; N, 11.58; S,6.63. Found: C, 59.50; H, 7.18; N, 11.97; S, 6.49.

*4.1.11.3. 5-(4-Phenylpiperidin-1-yl)-N-(3-methyl-2-oxo-2,3-dihydrobenzothiazol-6-yl)pentanamide **(11c)**.* Compound **11c** was obtained by using method B from intermediate **6** (600 mg, 3.3 mmol), 5-(4-phenylpiperidin-1-yl)pentanoic acid (967 mg, 3.6 mmol), EDC (767 mg, 4 mmol) and DMAP (81 mg, 0.7 mmol). Then it was recrystallized from 2-propanol. Yield: 340 mg, 24%; mp: 169.2 C. ^{1}H NMR (DMSO-d_6) δ: 9.96 (s, 1H, *N*–H), 7.95 (d, 1H, J = 2.4 Hz, H^7), 7.46 (dd, 1H, J = 8.8 Hz, J = 2.4 Hz, H^5), 7.26–7.12 (m, 6H, phenyl protons, H^4), 3.37 (s, 3H, *N*–CH$_3$), 2.92 (d, 2H, J = 11.5 Hz, H^{2e}, H^{6e}-piperidine), 2.49–2.26 (m, 5H, H^4-piperidine, -*N*-CH$_2$-CH$_2$-CH$_2$-CH$_2$-), 1.92 (td, 2H, J = 11.5 Hz, J = 2.4 Hz, H^{2a}, H^{6a}-piperidine), 1.70–1.54 (m, 6H, H^3, H^5-piperidine, -*N*–CH$_2$–CH$_2$-CH$_2$-CH$_2$-) 1.46 (p, 2H, J = 7.5 Hz, -*N*–CH$_2$–CH$_2$-CH$_2$-). ^{13}C NMR (DMSO-d_6) δ: 171.1, 168.3, 146.3, 135.1, 133.1, 128.2, 126.6, 125.9, 121.4, 117.9, 113.3, 111.2, 57.9, 53.8, 42.0, 33.1, 28.9, 26.1, 23.1. HRMS (ESI) [M+H]$^+$ *m/z* for $C_{24}H_{30}N_3O_2S$ calculated: 424.2059, found: 424.2048. Anal. Calcd. for $C_{24}H_{29}N_3O_2S$: C, 68.05; H, 6.90; N, 9.92; S, 7.55. Found: C, 68.10; H, 7.20; N, 9.90; S, 7.56.

*4.1.12. 6-(3-Chloropropanoyl)-3-methylbenzoxazol-2(3H)-one **(12)** and 6-(3-chloropropanoyl)-3-methylbenzothiazol-2(3H)-one **(13)***

6-(3-Chloropropanoyl)-3-methylbenzoxazol-2(3*H*)-one **(12)** and 6-(3-chloropropanoyl)-3-methylbenzothiazol-2(3*H*)-one **(13)** were synthesized according to the previously reported method [33]. Yield for **(12)**: 72%.; mp: 184 °C. HRMS (ESI) $[M+H]^+$ *m/z* for $C_{11}H_{10}ClNO_3$ calculated: 240.0427, found: 240.0423. Yield for **(13)**: 85%; mp: 132 °C. HRMS (ESI) $[M+H]^+$ *m/z* for $C_{11}H_{10}ClNO_2S$ calculated: 256.0199, found: 256.0192.

*4.1.13. General procedure for the preparation of 6-(3-substitutedpropanoyl)-3-methylbenzoxazol-2(3H)-one **(14a-c)** and 6-(3-substitutedpropanoyl)-3-methylbenzothiazol-2(3H)-one **(15a-c)** derivatives*

6-(3-Substitutedpropanoyl)-3-methylbenzoxazol-2(3*H*)-one **(14a)** and 6-(3-substitutedpropanoyl)-3-methylbenzothiazol-2(3*H*)-one **(14b** and **14c)** derivatives were synthesized by following method A as mentioned in section 4.1.5 from intermediate **12** or **13** (1 equivalent), the corresponding amine derivative (1.5 equivalent), NaI (3 equivalent) and K_2CO_3 (2.5 equivalent).

*4.1.13.1. 3-Methyl-6-(3-(4-benzylpiperazin-1-yl)propanoyl)benzoxazol-2(3H)-one **(14a)**.* The intermediate **12** (300 mg, 1.3 mmol) was treated with 1-benzylpiperazine (343 mg, 2 mmol) in the presence of NaI (563 mg, 3.9 mmol) and anhydrous potassium carbonate (456 mg, 3.3 mmol) according to method A then, it was recrystallized from ethanol. Yield: 202 mg, 43%; mp: 129.6 C. ^{1}H NMR (DMSO-d_6) δ: 7.93 (dd, 1H, J = 8.4 Hz, J = 1.6 Hz, H^5), 7.86 (d, 1H, J = 1.6 Hz, H^7), 7.34 (d, 1H, J = 8.4 Hz, H^4), 7.33–7.21 (m, 5H, phenyl protons), 3.43 (s, 2H, $-CH_2$-C_6H_5), 3.37 (s, 3H, *N*–CH_3), 3.16 (t, 2H, J = 7.2 Hz, $-CH_2$-CH_2-N), 2.65 (t, 2H, J = 7.2 Hz, -CH_2-CH_2-*N*-), 2.42–2.34 (m, 8H, H-piperazine). ^{13}C NMR (DMSO-d_6) δ: 197.6, 154.1, 141.8, 138.2, 135.9, 131.2, 128.7, 128.0, 126.8, 125.0, 108.7, 108.6, 62.0, 53.0, 52.6, 52.5, 35.6, 28.2. HRMS (ESI) $[M+H]^+$ *m/z* for $C_{22}H_{26}N_3O_3$ calculated: 380.1974, found: 380.1989. Anal. Calcd. for $C_{22}H_{25}N_3O_3$: C, 69.64; H, 6.64; N, 11.07. Found: C, 69.24; H, 6.84; N, 11.05.

*4.1.13.2. 3-Methyl-6-[3-(4-benzylpiperazin-1-yl)propanoyl]benzothiazol-2(3H)-one **(14b)**.* The intermediate **13** (300 mg, 1.2 mmol) was treated with 1-benzylpiperazine (317 mg, 1.8 mmol) in the presence of NaI (540 mg, 3.6 mmol) and anhydrous potassium carbonate (415 mg, 3 mmol) according to method A then, it was recrystallized from ethanol. Yield: 100 mg, 22%; mp: 99.9 C. ^{1}H NMR (DMSO-d_6) δ: 8.31 (d, 1H, J = 2.0 Hz, H^7), 7.97 (dd, 1H, J = 8.4 Hz, J = 2.0 Hz, H^5), 7.37 (d, 1H, J = 8.4 Hz, H^4), 7.30–7.18 (m, 5H, phenyl protons), 3.41 (s, 2H, $-CH_2$-C_6H_5), 3.40 (s, 3H, *N*–CH_3), 3.14 (t, 2H, J = 7.2 Hz, $-CH_2$-CH_2-N), 2.63 (t, 2H, J = 7.2 Hz, -CH_2-CH_2-*N*-), 2.40–2.32 (m, 8H, H-piperazine). ^{13}C NMR (DMSO-d_6) δ: 197.6, 169.3, 141.2, 138.2, 131.8, 128.7, 128.1, 126.9, 126.8, 123.2, 121.6, 111.0, 62.0, 53.0, 52.7, 52.6, 35.6, 29.2. HRMS (ESI) $[M+H]^+$ *m/z* for $C_{22}H_{26}N_3O_2S$ calculated: 396.1746, found: 396.1734. Anal. Calcd. for $C_{22}H_{25}N_3O_2S$: C, 66.81; H, 6.37; N, 10.62; S, 8.11. Found: C, 66.44; H, 6.54; N, 10.57; S, 7.95.

*4.1.13.3. 3-Methyl-6-[3-(4-phenylpiperidin-1-yl)propanoyl]benzothiazol-2(3H)-one **(14c)**.* The intermediate **13** (500 mg, 2 mmol) was treated with 1-phenylpiperidine (476 mg, 3 mmol) in the presence of NaI (900 mg, 6 mmol) and anhydrous potassium carbonate (691 mg, 5 mmol) according to method A then, it was recrystallized from acetone-hexane. Yield: 53 mg, 7%; mp: 103.7 C. ^{1}H NMR (DMSO-d_6) δ: 8.33 (d, 1H, J = 1.3 Hz, H^7), 8.30 (dd, 1H, J = 8.5 Hz, J = 1.3 Hz, H^5), 7.41 (d, 1H, J = 8.5 Hz, H^4), 7.30–7.15 (m, 5H, phenyl protons), 3.45 (s, 3H, *N*–CH_3), 3.22 (t, 2H, J = 7.2 Hz, $-CH_2$-CH_2-*N*-), 3.01 (d, 2H, J = 11.6 Hz, H^{2e}, H^{6e}-piperidine), 2.71 (t, 2H, J = 7.2 Hz, -CH_2-CH_2-*N*-), 2.51–2.42 (m, 1H, H^4-piperidine), 2.06 (td, 2H, J = 11.6 Hz, J = 2.1 Hz, H^{2a}, H^{6a}-piperidine), 1.76–1.50 (m, 4H, H^3, H^5-piperidine). ^{13}C NMR (DMSO-d_6) δ: 197.7, 169.3, 146.2, 141.2, 131.9, 128.2, 126.9, 126.6, 125.9, 123.1, 121.6, 111.0, 53.7, 53.3, 41.7, 35.8, 33.0, 29.2. HRMS (ESI) $[M+H]^+$ *m/z* for $C_{22}H_{25}N_2O_2S$ calculated: 381.1637, found: 381.1625. Anal. Calcd. for $C_{22}H_{24}N_2O_2S$: C, 69.44; H, 6.37; N, 7.36; S, 8.43. Found: C, 69.29; H, 6.77; N, 7.45; S, 8.73.

*4.1.14. 6-Nitrobenzothiazole **(15)***

Commercially available benzothiazole (3 g, 22 mmol) was taken to the flask and 6 ml 98% sulfuric acid was added in ice bath. After stirring for a while 65% nitric acid was added in portions. The experiment was completed by keeping the reaction mixture between 4 and 6 °C. The mixture was poured into ice water and the precipitated was filtered and recrystallized from ethanol. Yield: 33%, mp: 173–174 °C [34].

*4.1.15. 2-Amino-5-nitrobenzenethiol **(16)** (CAS 23451-98-1)*

15 (500 mg, 2.8 mmol) was refluxed with 30 ml 20% potassium hydroxide solution for 5 h. After the completion of the reaction, the mixture was cooled and neutralized with 37% HCl solution. The precipitate was collected by filtration and used in the next step without further purification. Yield: 59%, mp: 87–89 °C.

*4.1.16. 6-Nitro-2-phenylbenzoxazole **(17)** and 6-nitro-2-phenylbenzothiazole **(18)***

2-Amino-5-nitrophenol (commercially available) (1 g, 6.5 mmol) or 2-amino-5-nitrobenzenethiol **(16)** (1.1 g, 6.5 mmol) and (0.79 g, 6.5 mmol) benzoic acid were taken in a round bottom flask and covered with polyphosphoric acid. The reaction mixture was stirred in oil bath at 140 °C for 2 h. After this period, the mixture was cooled, poured into ice water, and then neutralized with sodium hydroxide solution. The precipitate was filtered, dried, and used in the next step. For (**17**) Yield: 90%, mp: 180 °C. For **(18)** Yield: 82%, mp: 188 °C [35].

*4.1.17. 6-Amino-2-phenylbenzoxazole **(19)** and 6-amino-2-phenylbenzothiazole **(20)***

The solution 6-nitro-2-phenylbenzoxazole **(17)** (0.9 g, 3.8 mmol) or 6-nitro-2-phenylbenzothiazole **(18)** (0.96 g, 3.8 mmol) in 40 ml ethanol was refluxed with 7 ml 1.2 N HCl. After starting reflux for a while, iron (0.6 g, 11 mmol) was added and stirred under reflux condition till the completion of reaction. Then the reaction mixture was filtered through Celite® to remove iron. The filtrate was taken and made alkaline with sodium hydroxide solution. The precipitate was filtered and used without further purification. Yield for **(19)**: 48%, mp: 173 °C. Yield for **(20)**: 40%, mp: 206 °C [35].

*4.1.18. General procedure for the preparation of compounds **21a** and **21b***

3-(4-Benzylpiperazin-1-yl)-*N*-(2-phenylbenzoxazol-6-yl)propanamide **(21a)** and 3-(4-benzylpiperazin-1-yl)-*N*-(2-phenylbenzothiazol-6-yl)propanamide **(21b)** were synthesized by method B as mentioned in section 4.1.7 from intermediate **19** or **20** (1 equivalent), 3-(4-benzylpiperazine-1-yl)propanoic acid (1.1 equivalent), EDC (1.2 equivalent) and DMAP (0.2 equivalent).

*4.1.18.1. 3-(4-Benzylpiperazin-1-yl)-N-(2-phenylbenzoxazol-6-yl) propanamide **(21a)**.* Compound **21a** was obtained by using method B from intermediate **19** (450 mg, 2.1 mmol), 3-(4-benzylpiperazin-1-yl)propanoic acid (585 mg, 2.4 mmol), EDC (493 mg, 2.6 mmol) and DMAP (52 mg, 0.4 mmol). Then it was recrystallized from acetone-hexane. Yield: 155 mg, 16%; mp: 139.5 C. ^{1}H NMR (DMSO-d_6) δ: 10.37 (s, 1H, *N*–H), 8.25 (s, 1H, H^7), 8.18–8.15 (m, 2H,

$H^{2'}$, $H^{6'}$), 7.70 (d, 1H, J = 8.4 Hz, H^4), 7.61–7.58 (m, 3H, $H^{3'}$, $H^{4'}$, $H^{5'}$), 7.37 (dd, 1H, J = 8.4 Hz, J = 1.6 Hz, H^5), 7.32–7.21 (m, 5H, phenyl protons), 3.44 (s, 2H, $-CH_2$-C_6H_5), 2.65 (t, 2H, J = 6.4 Hz, -*N*-CH_2-CH_2-), 2.50–2.47 (m, 2H, -*N*–CH_2–CH_2-, with DMSO), 2.45–2.38 (m, 8H, piperazine). ^{13}C NMR (DMSO-d_6) δ: 170.3, 161.8, 150.3, 138.1, 137.1, 136.8, 131.5, 129.1, 128.7, 128.0, 126.9, 126.7, 126.4, 119.5, 116.4, 101.1, 61.9, 53.5, 52.5, 52.3, 34.1. HRMS (ESI) $[M+H]^+$ m/z for $C_{27}H_{29}N_4O_2$ calculated: 441.2291, found: 441.2275. Anal. Calcd. for $C_{27}H_{28}N_4O_2$: C, 73.61; H, 6.41; N, 12.72. Found: C, 73.42; H, 6.75; N, 12.73.

4.1.18.2. 3-(4-Benzylpiperazin-1-yl)-N-(2-phenylbenzothiazol-6-yl) propanamide ***(21b)****.* Compound **21b** was obtained by using method B from intermediate **20** (400 mg, 1.7 mmol), 3-(4-benzylpiperazin-1-yl)propanoic acid (483 mg, 1.9 mmol), EDC (407 mg, 2.1 mmol) and DMAP (43 mg, 0.3 mmol). Then it was recrystallized from acetone-hexane. Yield: 200 mg, 25%; mp: 162.9 C. ^{1}H NMR (DMSO-d_6) δ: 10.36 (s, 1H, *N*–H), 8.51 (d, 1H, J = 1.2 Hz, H^7), 8.04–8.01 (m, 2H, $H^{2'}$, $H^{6'}$), 7.95 (d, 1H, J = 8.8 Hz, H^4), 7.54–7.50 (m, 4H, H^5, $H^{3'}$, $H^{4'}$,$H^{5'}$), 7.31–7.19 (m, 5H, phenyl protons), 3.42 (s, 2H, $-CH_2$-C_6H_5), 2.63 (t, 2H, J = 7.0 Hz, -*N*-CH_2-CH_2-), 2.50–2.47 (m, 2H, -*N*–CH_2–CH_2-, with DMSO), 2.42–2.36 (m, 8H, piperazine). ^{13}C NMR (DMSO-d_6) δ: 170.3, 165.5, 149.3, 138.1, 136.9, 135.1, 132.8, 131.0, 129.2, 128.7, 128.0, 126.8, 126.7, 122.8, 118.8, 111.1, 61.9, 53.6, 52.5, 52.3, 34.0. HRMS (ESI) $[M+H]^+$ m/z for $C_{27}H_{29}N_4OS$ calculated: 457.2062, found: 457.2078. Anal. Calcd. for $C_{27}H_{28}N_4OS$: C, 71.02; H, 6.18; N, 12.27; S, 7.02. Found: C, 70.62; H, 6.48; N, 12.26; S, 7.06.

4.2. Biological studies

4.2.1. Cholinesterase inhibition assay

AChE and BChE % inhibitory activities of the 42 test compounds at 100 μM concentration were determined by the modified Ellman's method and compounds displaying more than 50% inhibition were tested for IC_{50} determination. The formation of the yellow color was measured at 412 nm using molecular devices, Versamax microplate reader. Electric eel AChE (type-VI-S, EC 3.1.1.7), recombinant human AChE, equine serum BChE (EC 3.1.1.8), recombinant human BChE, 5,5′-dithiobis-2-nitrobenzoic acid (DTNB), acetylthiocholine iodide (ATI), butyrylthiocholine iodide (BTI) and Tris HCl were purchased from Sigma Aldrich. Donepezil and Galantamine were used as the reference drug at 10 μM concentration. Sample compounds were dissolved in DMSO (DMSO was 1% and has no inhibitory effect at this amount). For AChE inhibitory activity tested, in each well of the plate were contained 168 μL of 50 mM of Tris HCl buffer (pH 8.0), 10 μL of 6.8 mM DTNB solution, 10 μL of AChE solution (0.4 U/mL), and 2 μL of each sample solution and incubated for 10 min at 25 °C. Then the reactions were initiated by the addition of 10 μL ATI solution (10 mM). Changes in absorbance was recorded for 10 min at 412 nm. As a control, an identical solution of the reaction mixture without the sample solution was processed following the same protocol. The blank reading contained 178 μL buffer, 10 μL DTNB, 2 μL DMSO and 10 μL ATI solution. BChE inhibitory activities of the test compounds were measured through the same methodology described, except employing 0.8 U/mL BChE solution as the enzyme source and the BTI solution (30 mM) as the substrate of the reaction. Each experiment was performed in triplicate; absorbance values were corrected by subtracting the absorbance of blank and the inhibition rate (%) was calculated. To determine the IC_{50} values, graphic from log [inhibitor] vs. % inhibition was analyzed with the use of GraphPad Prism software (Version 7.0). The results were displayed as mean ± SD [29,30].

4.2.2. Reversibility studies for AChE/BuChE inhibition

Reversibility studies were carried with the dilution method using modified Ellman's method for the measurement of residual enzyme activities of dilutions [36]. The enzyme AChE/BChE (0.5 U/mL), ATI/BTI (0.01 M) and DTNB (0.01 M) were diluted in tris-HCl buffer (pH-8). Briefly, 10 × IC_{50} and 100 × IC_{50} concentrations of these inhibitors were incubated with 40 μL of diluted enzyme at 37 °C for 30 min, then 20 μL of DTNB solution was added. After this incubation period, the reaction was subsequently diluted 100-fold with substrate solution to give final concentrations of inhibitors 0.1 × IC_{50} and 1 × IC_{50}, respectively. In control studies, inhibitors were replaced with donepezil or buffer. The reaction was further incubated at 37 °C for a further 15 min and the residual enzyme activities were measured, and the bar graphs were constructed. All measurements were carried out in triplicate and are expressed as mean ± SEM.

4.2.3. Kinetic characterization of cholinesterase inhibition

Enzyme kinetic studies were performed similar as enzyme inhibition assay. The increase of the absorbances was measured with different inhibitor concentrations and without inhibitor for proposed substrate concentrations. To determine the inhibition model, reciprocal plots of 1/V versus 1/[S] were constructed by using reported method with minor modifications. Slopes of the reciprocal plots were plotted against the concentration of inhibitor, for estimation of Ki. All processes were assayed in triplicate and data analysis was performed with GraphPad Prism software (Version 7.0). The results were displayed as mean ± SD [29,30].

4.2.4. Oxygen radical absorbance capacity (ORAC-Fluorescein) assay

The antioxidant activity was determined by the oxygen radical absorbance capacity fluorescein (ORAC-FL) method [40,41]. Each assay was conducted with 75 mM phosphate buffer (pH 7.4), and the final reaction mixture was 200 μL. Test samples (20 μL) and fluorescein (120 μL, 150 nM final concentration) were placed in the wells of a black 96-well plate. The mixture was pre-incubated for 15 min at 37 °C, and then AAPH (i.e., 2,2′- azobis(2-methylpropionamidine) dihydrochloride (AAPH) solution (60 μL, 12 mM final concentration) was added rapidly using an autosampler. The plate was immediately placed in a Varioskan Flash Multimode Reader (Thermo Scientific) and the fluorescence recorded every minute for 90 min with excitation at 485 nm and emission at 535 nm. The plate was automatically shaken prior to each reading. Trolox was used as standard (0.5–8 μM, final concentration). A blank (FL + AAPH) using phosphate buffer instead of antioxidant and trolox calibration were carried out in each assay. The samples were measured at 10 μM concentration. All the reaction mixture was prepared in duplicate, and three independent assays were performed for each sample. Antioxidant curves (fluorescence versus time) were normalized to the curve of the blank in the same assay, and then the area under the fluorescence decay curve (AUC) was calculated. The net AUC of a sample was obtained by subtracting the AUC of the blank. ORACFL values were expressed as Trolox equivalents by using the standard curve calculated for each sample, where the ORAC-FL value of Trolox was taken as 1, indicating the antioxidant potency of the tested compounds.

4.2.5. Inhibiting inflammatory factors production of LPS-stimulated THP1 cells

4.2.5.1. Cell culture and LPS stimulation of THP1 cells. The THP1 cell line was obtained from Sigma by Atlas Biotechnology, and cultured in complete medium (RPMI 1640 medium supplemented with 10% FCS, 100 U/mL penicillin, and 100 μg/ml streptomycin) at 37 °C in a humidified incubator containing 5% CO_2. After overnight culture in 24-well plate (4 × 10^4 cells/well), the cells were treated with or without 10 μM concentration of compound that were added 1 h

prior to with 100 ng/ml LPS from *Escherichia coli* serotype O111:B4 (Sigma Aldrich, USA) for 24 h. Untreated cells were used as a negative control. Cells treated with LPS were used as an inflammation positive group. After 24 h, to determine the effect of selected compounds on cytokine levels from experimental test group. All experiments were at least in triplicate [42,43].

4.2.5.2. Nitric oxide (NO) production and cytokine measurement. After overnight culture in a 24-well plate (4×10^4 cells/well, 500 μL medium/well), the cells were treated with or without various concentrations of madde isimleri that were added 1 h prior to with 100 ng/ml LPS from *Escherichia coli* serotype O111:B4 (Sigma Aldrich, USA) for 24 h. After incubation period, Cell-free supernatants were collected and stored at −20 °C until assayed for NO levels. The concentrations of NO in the supernatants of THP1 cell cultures were determined using an ELISA kit, according to the manufacturer's instructions (Bt-Laboratory). Total protein extraction from the cell pellets according to the GeneALL ProtinExTM Animal cell/tissue Protein Isolation Kit (GeneALL Biotechnology). Human Interleukin 1 Beta, Human Interleukin 6, and Human Tumor Necrosis Factor Alpha (Bt-Laboratory) levels of protein samples were measured by enzyme immunoassay (EIA). Absorbance readings were carried out 450 nm using Microplate Reader (Thermo Fisher Scientific, Finland). Concentrations of unknown samples were determined from a standard curve obtained with the standards. According to the kit protocol, the sensitivities were 10,07 pg/ml, 1,03 ng/l, 1,52 ng/l, and 1,12 μmol/l for Human Interleukin 1 Beta, Human Interleukin 6, Human Tumor Necrosis Factor Alpha, and Human Nitric Oxide respectively [43].

4.2.6. Aβ aggregation inhibition assay/thioflavin T (ThT) assay

All the chemicals used for the assay purchased from Sigma-Aldrich and measurements carried out at Thermo Biolite 24 well multidish plate by using SpectraMax i3x Multi-Mode microplate reader. To investigate the effect of the selected compounds and references (Donepezil and phenol red) on the aggregation of $A\beta_{1-42}$ at 50 mM concentration, a reported thioflavin T-based fluorometric assay was performed. Samples were dissolved in DMSO and analyzed in triplicate [44].

4.2.7. Annexin V-FITC/PI apoptosis measurement

Annexin V/PI binding assay based on the cell membrane externalization of phosphatidylserine, apoptosis detection procedure [45,46]. 3T3 fibroblast cells were treated with 10 μM concentrations of compounds for 24 h. After incubation period, control and test groups were trypsinized, washed PBS and cells were stained with Annexin V conjugated with FITC and PI using the Annexin V-FITC/PI Apoptosis Detection Kit (BD Pharmingen, USA), according to the manufacturer's protocols. Then, viable and apoptotic cells were analyzed with the BD Accuri C6 Flow Cytometer (BD Bioscience, USA). Untreated cells served as a negative control.

4.2.8. Cell culture and cell proliferation test (MTT assay)

3T3 fibroblast cell line (ATCC CCL92) was kindly provided by Sap Institute Cell Bank. The cells were cultured as adherent monolayers in T25 tissue culture plates in DMEM supplemented with 10% inactivated fetal bovine serum (Sigma-Aldrich, USA), 2 mM l-glutamine, 100 U/mL penicillin, and 100 mg/ml streptomycin at 37 °C in a humidified incubator containing 5% CO_2. The cells incubated with selected compounds at concentrations 0.1−10 μM. At the end of 24 h, the cell viability was determined MTT (3-(4,5-dimethylthiazol-2-yl)-2,5-diphenyl tetrazolium bromide) Cell Proliferation Kit (Roche Diagnostics, Germany) according to the manufacturer's protocol. 10 μl of MTT solution was added to wells and plates were incubated in a humidified atmosphere of 5% CO_2 in air at 37 °C for 4 h. After the incubation, the supernatant was removed, the formazan crystals were dissolved in 0.1 ml of SDS and the plates were incubated for 24 h. Then, the optical densities were read at 570 nm in multi-well spectrophotometer (Thermo Fisher Scientific, Finland). The relative cell viability of the test group was calculated using the following formula: relative cell viability of the test group (%) = (optical density of the test group/optical density of the untreated group) × 100. All controls and test groups were performed at least in triplicates [29,30].

4.2.9. Statistical analysis

According to the experimental design, at least 3 independent experiments were performed, and the data were presented as means ± standard deviation (means ± SD) values. One-way ANOVA with post hoc analysis by using Tukey comparison test was performed for multiple comparisons between groups. P value < 0.05 was considered as statistically significant. Statistics were evaluated using SPSS 17.0.

4.3. Assessment of physicochemical parameters

Calculated descriptors (molecular weight, log P, topological polar surface area (tPSA), volume, number of hydrogen donors, number of hydrogen acceptors and number of violations of Lipinski's rule) of the compounds were computed employing the Molinspiration online service [47]. Blood brain barrier (BBB) permeability values were calculated by admetSAR online service [48].

4.4. Molecular modeling studies

Before the molecular docking, the geometry of the initial structures of ligands considered was optimized by using the Gaussian 09 software [49] with the semi-empirical parametric method 6 (PM6) [50]. The crystal structures of the AChE and BChE enzymes were retrieved from the RCSB Protein Data Bank (http://www.rcsb.org/pdb/), under the accession codes 1EVE [39] and 4BDS [51], respectively. Molecular Operating Environment (MOE) v2014.0901 [52] was used for molecular docking studies. The co-crystallized bound compounds and water molecules farther than 4.5 Å from ligand or receptor were deleted from the crystal structure. Water molecules closer than 4.5 Å were conserved since water-mediated contacts were reported as crucial for binding and specificity [39]. Enzyme-ligand complexes were energy minimized to a gradient of 0.01 kcal/(mol Å), and protonated by means of the force field AMBER99. Charges on the enzyme and ligands were assigned using the force fields AMBER99 and MMF94X, correspondingly. Possible ligand-binding sites were identified by the "Site Finder" module of the MOE. For each ligand, Triangle Matcher Algorithm and scoring function of London dG was used for ranking 1000 docked poses. Then a force field refinement at default parameters was carried out for the 30 poses followed by a rescoring of GBVI/WSA dG. All poses generated with docking were analyzed and the best-scored pose with the lowest binding free energy for each compound was selected for further investigation of interactions with the corresponding enzyme.

The docking procedure was validated by re-docking the co-crystallized ligands of AChE and BChE. The most energetically stable ligand poses obtained by re-docking were largely similar with the ligands in the crystal structure of enzymes with the root mean square deviation (RMSD) values of 0.196 Å for AChE and 0.149 Å for BChE.

Declaration of competing interest

The authors declare that they have no known competing financial interests or personal relationships that could have appeared to influence the work reported in this paper.

The authors declare no conflict of interest.

Acknowledgments

This work was supported by the Scientific and Technological Research Council of Turkey (TUBITAK) [grant number 115S192].

Appendix A. Supplementary data

Supplementary data to this article can be found online at https://doi.org/10.1016/j.ejmech.2020.113124.

References

[1] A. Alzheimer's, Alzheimer's disease facts and figures, Alzheimers, Dementia 12 (2016) 459–509, https://doi.org/10.1016/j.jalz.2016.03.001, 2016.
[2] World Alzheimer Report 2019: Attitudes to Dementia, Alzheimer's Disease International, 2019, pp. 1–13.
[3] K.G. Yiannopoulou, S.G. Papageorgiou, Current and future treatments for Alzheimer's disease, Ther. Adv. Neurol. Disord. 6 (2012) 19–33, https://doi.org/10.1177/1756285612461679.
[4] A. Kumar, A. Singh, Ekavali, A review on Alzheimer's disease pathophysiology and its management: an update, Pharmacol. Rep. 67 (2015) 195–203, https://doi.org/10.1016/j.pharep.2014.09.004.
[5] F. Zemek, L. Drtinova, E. Nepovimova, V. Sepsova, J. Korabecny, J. Klimes, K. Kuca, Outcomes of Alzheimer's disease therapy with acetylcholinesterase inhibitors and memantine, Expet Opin. Drug Saf. 13 (2014) 759–774, https://doi.org/10.1517/14740338.2014.914168.
[6] J. Korabecny, F. Zemek, O. Soukup, K. Spilovska, K. Musilek, D. Jun, E. Nepovimova, K. Kuca, Chapter 1 - pharmacotherapy of Alzheimer's disease: current state and future perspectives, in: R. Atta ur, M.I. Choudhary (Eds.), Drug Design and Discovery in Alzheimer's Disease, Elsevier, 2014, pp. 3–39.
[7] C.B. Mishra, S. Kumari, A. Manral, A. Prakash, V. Saini, A.M. Lynn, M. Tiwari, Design, synthesis, in-silico and biological evaluation of novel donepezil derivatives as multi-target-directed ligands for the treatment of Alzheimer's disease, Eur. J. Med. Chem. 125 (2017) 736–750, https://doi.org/10.1016/j.ejmech.2016.09.057.
[8] J.W. Kinney, S.M. Bemiller, A.S. Murtishaw, A.M. Leisgang, A.M. Salazar, B.T. Lamb, Inflammation as a central mechanism in Alzheimer's disease, Alzheimers. Dement. 4 (2018) 575–590, https://doi.org/10.1016/j.trci.2018.06.014.
[9] J.M. Rubio-Perez, J.M. Morillas-Ruiz, A review: inflammatory process in Alzheimer's disease, role of cytokines, Sci. World J. 2012 (2012), 756357, https://doi.org/10.1100/2012/756357.
[10] M. Marttinen, M. Takalo, T. Natunen, R. Wittrahm, S. Gabbouj, S. Kemppainen, V. Leinonen, H. Tanila, A. Haapasalo, M. Hiltunen, Molecular mechanisms of synaptotoxicity and neuroinflammation in Alzheimer's disease, Front. Neurosci. 12 (2018) 963, https://doi.org/10.3389/fnins.2018.00963.
[11] M.T. Heneka, M.J. Carson, J. El Khoury, G.E. Landreth, F. Brosseron, D.L. Feinstein, A.H. Jacobs, T. Wyss-Coray, J. Vitorica, R.M. Ransohoff, K. Herrup, S.A. Frautschy, B. Finsen, G.C. Brown, A. Verkhratsky, K. Yamanaka, J. Koistinaho, E. Latz, A. Halle, G.C. Petzold, T. Town, D. Morgan, M.L. Shinohara, V.H. Perry, C. Holmes, N.G. Bazan, D.J. Brooks, S. Hunot, B. Joseph, N. Deigendesch, O. Garaschuk, E. Boddeke, C.A. Dinarello, J.C. Breitner, G.M. Cole, D.T. Golenbock, M.P. Kummer, Neuroinflammation in Alzheimer's disease, Lancet Neurol. 14 (2015) 388–405, https://doi.org/10.1016/S1474-4422(15)70016-5.
[12] Q.-q. Yang, J.-w. Zhou, Neuroinflammation in the central nervous system: symphony of glial cells, Glia 67 (2019) 1017–1035, https://doi.org/10.1002/glia.23571.
[13] A. Ardura-Fabregat, E.W.G.M. Boddeke, A. Boza-Serrano, S. Brioschi, S. Castro-Gomez, K. Ceyzériat, C. Dansokho, T. Dierkes, G. Gelders, M.T. Heneka, L. Hoeijmakers, A. Hoffmann, L. Iaccarino, S. Jahnert, K. Kuhbandner, G. Landreth, N. Lonnemann, P.A. Löschmann, R.M. McManus, A. Paulus, K. Reemst, J.M. Sanchez-Caro, A. Tiberi, A. Van der Perren, A. Vautheny, C. Venegas, A. Webers, P. Weydt, T.S. Wijasa, X. Xiang, Y. Yang, Targeting neuroinflammation to treat Alzheimer's disease, CNS Drugs 31 (2017) 1057–1082, https://doi.org/10.1007/s40263-017-0483-3.
[14] M. Rekatsina, A. Paladini, A. Piroli, P. Zis, J.V. Pergolizzi, G. Varrassi, Pathophysiology and therapeutic perspectives of oxidative stress and neurodegenerative diseases: a narrative review, Adv. Ther. 37 (2020) 113–139, https://doi.org/10.1007/s12325-019-01148-5.
[15] A. Singh, R. Kukreti, L. Saso, S. Kukreti, Oxidative stress: a key modulator in neurodegenerative diseases, Molecules 24 (2019), https://doi.org/10.3390/molecules24081583.
[16] P. Poprac, K. Jomova, M. Simunkova, V. Kollar, C.J. Rhodes, M. Valko, Targeting free radicals in oxidative stress-related human diseases, Trends Pharmacol. Sci. 38 (2017) 592–607, https://doi.org/10.1016/j.tips.2017.04.005.
[17] P. Jacques, C. Pascal, C. Evelina, 2(3*H*)-Benzoxazolone and bioisosters as "privileged scaffold" in the design of pharmacological probes, Curr. Med. Chem. 12 (2005) 877–885, https://doi.org/10.2174/0929867053507388.
[18] D.S. Doğruer, S. Ünlü, E. Yeşilada, M.F. Şahin, N-(2-pyridinyl)-2-[2(3H)-benzazolone-3-yl]acetamides: synthesis, antinociceptive and anti-inflammatory activity, Farmaco 52 (1997) 745–750.
[19] A.H. Abdelazeem, S.I. Khan, S.W. White, K.J. Sufka, C.R. McCurdy, Design, synthesis and biological evaluation of bivalent benzoxazolone and benzothiazolone ligands as potential anti-inflammatory/analgesic agents, Bioorg. Med. Chem. 23 (2015) 3248–3259, https://doi.org/10.1016/j.bmc.2015.04.057.
[20] D.S. Doğruer, S. Ünlü, M.F. Şahin, E. Yeşilada, Anti-nociceptive and anti-inflammatory activity of some (2-benzoxazolone-3-yl and 2-benzothiazolone-3-yl) acetic acid derivatives, Il Farmaco 53 (1998) 80–84, https://doi.org/10.1016/S0014-827X(97)00017-7.
[21] O. Gulcan, S. Ünlü, E. Banoglu, M.F. Şahin, E. Yesilada, Synthesis of new 4-(5-chloro-2-oxo-3H-benzoxazol-3-yl) butanamide derivatives and their analgesic and anti-inflammatory properties, Turk. J. Chem. 27 (2003) 467–476.
[22] H. Aichaoui, F. Guenadil, C.N. Kapanda, D.M. Lambert, C.R. McCurdy, J.H. Poupaert, Synthesis and pharmacological evaluation of antioxidant chalcone derivatives of 2(3H)-benzoxazolones, Med. Chem. Res. 18 (2009) 467–476, https://doi.org/10.1007/s00044-008-9143-y.
[23] H. Akrami, B.F. Mirjalili, M. Khoobi, H. Nadri, A. Moradi, A. Sakhteman, S. Emami, A. Foroumadi, A. Shafiee, Indolinone-based acetylcholinesterase inhibitors: synthesis, biological activity and molecular modeling, Eur. J. Med. Chem. 84 (2014) 375–381, https://doi.org/10.1016/j.ejmech.2014.01.017.
[24] P.N. Tripathi, P. Srivastava, P. Sharma, M.K. Tripathi, A. Seth, A. Tripathi, S.N. Rai, S.P. Singh, S.K. Shrivastava, Biphenyl-3-oxo-1,2,4-triazine linked piperazine derivatives as potential cholinesterase inhibitors with anti-oxidant property to improve the learning and memory, Bioorg. Chem. 85 (2019) 82–96, https://doi.org/10.1016/j.bioorg.2018.12.017.
[25] L. Jalili-Baleh, E. Babaei, S. Abdpour, S. Nasir Abbas Bukhari, A. Foroumadi, A. Ramazani, M. Sharifzadeh, M. Abdollahi, M. Khoobi, A review on flavonoid-based scaffolds as multi-target-directed ligands (MTDLs) for Alzheimer's disease, Eur. J. Med. Chem. 152 (2018) 570–589, https://doi.org/10.1016/j.ejmech.2018.05.004.
[26] A. Cavalli, M.L. Bolognesi, A. Minarini, M. Rosini, V. Tumiatti, M. Recanatini, C. Melchiorre, Multi-target-Directed ligands to combat neurodegenerative diseases, J. Med. Chem. 51 (2008) 347–372, https://doi.org/10.1021/jm7009364.
[27] C. Yamalı, H.O. Gülcan, B. Kahya, S. Çobanoğlu, M.K. Şüküroğlu, D.S. Doğruer, Synthesis of some 3(2H)-pyridazinone and 1(2H)-phthalazinone derivatives incorporating aminothiazole moiety and investigation of their antioxidant, acetylcholinesterase, and butyrylcholinesterase inhibitory activities, Med. Chem. Res. 24 (2015) 1210–1217, https://doi.org/10.1007/s00044-014-1205-8.
[28] B. Kılıç, H.O. Gülcan, M. Yalçın, F. Aksakal, A. Dimoglo, M.F. Şahin, D.S. Doğruer, Synthesis of some new 1(2H)-Phthalazinone derivatives and evaluation of their acetylcholinesterase and butyrylcholinesterase inhibitory activities, Lett. Drug Des. Discov. 14 (2017) 159–166, https://doi.org/10.2174/1570180813666160819124611.
[29] B. Kılıç, H.O. Gülcan, F. Aksakal, T. Erçetin, N. Oruklu, E. Ümit Bagriacik, D.S. Doğruer, Design and synthesis of some new carboxamide and propanamide derivatives bearing phenylpyridazine as a core ring and the investigation of their inhibitory potential on in-vitro acetylcholinesterase and butyrylcholinesterase, Bioorg. Chem. 79 (2018) 235–249, https://doi.org/10.1016/j.bioorg.2018.05.006.
[30] B. Kılıç, M. Erdoğan, H.O. Gülcan, F. Aksakal, N. Oruklu, E.U. Bağrıaçık, D.S. Doğruer, Design, synthesis and investigation of new diphenyl substituted pyridazinone derivatives as both cholinesterase and aβ-aggregation inhibitors, Med. Chem. 15 (2019) 59–76, https://doi.org/10.2174/1573406414666180524073241.
[31] Y. Gülkok, T. Biçer, F.K. Onurdağ, S. Özgen, M.F. Şahin, D.S. Doğruer, Synthesis of some new urea and thiourea derivatives and evaluation of their antimicrobial activities, Turk. J. Chem. 36 (2012) 279–291, https://doi.org/10.3906/kim-1106-54.
[32] A.S. Ünal, F.K. Onurdağ, S. Özgen, D. Doğruer, T. Önkol, Studies on the synthesis of 3-methyl-6-(substituted-urea/-thiourea)-2(3H)-benzothiazolone derivatives and antimicrobial activities, Indian J. Chem., Sect. B 54 (2015) 253–259.
[33] H. Aichaoui, D. Lesieur, J.-P. Hénichart, A Convenient and efficient method for the preparation of 6-Acyl-2(3H)-benzoxazolones, J. Heterocycl. Chem. 29 (1992) 171–175, https://doi.org/10.1002/jhet.5570290131.
[34] P. Hrobárik, V. Hrobáriková, I. Sigmundová, P. Zahradník, M. Fakis, I. Polyzos, P. Persephonis, Benzothiazoles with tunable electron-withdrawing strength and reverse polarity: a route to triphenylamine-based chromophores with enhanced two-photon absorption, J. Org. Chem. 76 (2011) 8726–8736, https://doi.org/10.1021/jo201411t.
[35] C.-X. Wei, D. Wu, Z.-G. Sun, K.-Y. Chai, Z.-S. Quan, Synthesis of 6-(3-substituted-4H-1,2,4-triazol-4-yl)-2-phenylbenzo[d]oxazoles as potential anticonvulsant agents, Med. Chem. Res. 19 (2010) 925–935, https://doi.org/

10.1007/s00044-009-9239-z.
[36] V. Kumar, B. Kumar, A. Ranjan Dwivedi, D. Mehta, N. Kumar, B. Bajaj, T. Arora, V. Prashar, J. Parkash, V. Kumar, Design, synthesis and evaluation of O-pentyne substituted diphenylpyrimidines as monoamine oxidase and acetylcholinesterase inhibitors, Chemistry 5 (2020) 8021–8032, https://doi.org/10.1002/slct.202002425.
[37] S. Mostert, W. Mentz, A. Petzer, J.J. Bergh, J.P. Petzer, Inhibition of monoamine oxidase by 8-[(phenylethyl)sulfanyl]caffeine analogues, Bioorg. Med. Chem. 20 (2012) 7040–7050, https://doi.org/10.1016/j.bmc.2012.10.005.
[38] M. Arikawa, Y. Kakinuma, T. Noguchi, H. Todaka, T. Sato, Donepezil, an acetylcholinesterase inhibitor, attenuates LPS-induced inflammatory response in murine macrophage cell line RAW 264.7 through inhibition of nuclear factor kappa B translocation, Eur. J. Pharmacol. 789 (2016) 17–26, https://doi.org/10.1016/j.ejphar.2016.06.053.
[39] G. Kryger, I. Silman, J.L. Sussman, Structure of acetylcholinesterase complexed with E2020 (Aricept): implications for the design of new anti-Alzheimer drugs, Structure 7 (1999) 297–307, https://doi.org/10.1016/S0969-2126(99)80040-9.
[40] X. Yang, X. Qiang, Y. Li, L. Luo, R. Xu, Y. Zheng, Z. Cao, Z. Tan, Y. Deng, Pyridoxine-resveratrol hybrids Mannich base derivatives as novel dual inhibitors of AChE and MAO-B with antioxidant and metal-chelating properties for the treatment of Alzheimer's disease, Bioorg. Chem. 71 (2017) 305–314, https://doi.org/10.1016/j.bioorg.2017.02.016.
[41] A. Dávalos, C. Gómez-Cordovés, B. Bartolomé, Extending applicability of the oxygen radical absorbance capacity (ORAC−Fluorescein) assay, J. Agric. Food Chem. 52 (2004) 48–54, https://doi.org/10.1021/jf0305231.
[42] M.M. Tucureanu, D. Rebleanu, C.A. Constantinescu, M. Deleanu, G. Voicu, E. Butoi, M. Calin, I. Manduteanu, Lipopolysaccharide-induced inflammation in monocytes/macrophages is blocked by liposomal delivery of G(i)-protein inhibitor, Int. J. Nanomed. 13 (2017) 63–76, https://doi.org/10.2147/IJN.S150918.
[43] L.W. Soromou, Z. Zhang, R. Li, N. Chen, W. Guo, M. Huo, S. Guan, J. Lu, X. Deng, Regulation of inflammatory cytokines in lipopolysaccharide-stimulated RAW 264.7 murine macrophage by 7-O-Methyl-naringenin, Molecules 17 (2012), https://doi.org/10.3390/molecules17033574.
[44] M.L. Bolognesi, V. Andrisano, M. Bartolini, R. Banzi, C. Melchiorre, Propidium-based polyamine ligands as potent inhibitors of acetylcholinesterase and acetylcholinesterase-induced amyloid-beta aggregation, J. Med. Chem. 48 (2005) 24–27, https://doi.org/10.1021/jm049156q.
[45] I. Vermes, C. Haanen, H. Steffens-Nakken, C. Reutellingsperger, A novel assay for apoptosis Flow cytometric detection of phosphatidylserine expression on early apoptotic cells using fluorescein labelled Annexin V, J. Immunol. Methods 184 (1995) 39–51, https://doi.org/10.1016/0022-1759(95)00072-I.
[46] M. van Engeland, L.J.W. Nieland, F.C.S. Ramaekers, B. Schutte, C.P.M. Reutelingsperger, Annexin V-Affinity assay: a review on an apoptosis detection system based on phosphatidylserine exposure, Cytometry 31 (1998) 1–9, https://doi.org/10.1002/(SICI)1097-0320(19980101)31:1<1:AID-CYTO1>3.0.CO;2-R.
[47] Molinspiration, Molinspiration cheminformatics nova ulica SK-900 26 slovensky grob Slovak republic. https://www.molinspiration.com/.
[48] F. Cheng, W. Li, Y. Zhou, J. Shen, Z. Wu, G. Liu, P.W. Lee, Y. Tang, admetSAR: a comprehensive source and free tool for assessment of chemical admet properties, J. Chem. Inf. Model. 52 (2012) 3099–3105, https://doi.org/10.1021/ci300367a.
[49] M.J. Frisch, G.W. Trucks, H.B. Schlegel, G.E. Scuseria, M.A. Robb, J.R. Cheeseman, G. Scalmani, V. Barone, B. Mennucci, G.A. Petersson, H. Nakatsuji, M. Caricato, X. Li, H.P. Hratchian, A.F. Izmaylov, J. Bloino, G. Zheng, J.L. Sonnenberg, M. Hada, M. Ehara, K. Toyota, R. Fukuda, J. Hasegawa, M. Ishida, T. Nakajima, Y. Honda, O. Kitao, H. Nakai, T. Vreven, J.A. Montgomery Jr., J.E. Peralta, F. Ogliaro, M.J. Bearpark, J. Heyd, E.N. Brothers, K.N. Kudin, V.N. Staroverov, R. Kobayashi, J. Normand, K. Raghavachari, A.P. Rendell, J.C. Burant, S.S. Iyengar, J. Tomasi, M. Cossi, N. Rega, N.J. Millam, M. Klene, J.E. Knox, J.B. Cross, V. Bakken, C. Adamo, J. Jaramillo, R. Gomperts, R.E. Stratmann, O. Yazyev, A.J. Austin, R. Cammi, C. Pomelli, J.W. Ochterski, R.L. Martin, K. Morokuma, V.G. Zakrzewski, G.A. Voth, P. Salvador, J.J. Dannenberg, S. Dapprich, A.D. Daniels, Ö. Farkas, J.B. Foresman, J.V. Ortiz, J. Cioslowski, D.J. Fox, Gaussian 09, Gaussian, Inc., Wallingford, CT, USA, 2009.
[50] J.J. Stewart, Optimization of parameters for semiempirical methods I. Method, J. Comput. Chem. 10 (1989) 209–220, https://doi.org/10.1007/s00894-012-1667-x.
[51] F. Nachon, E. Carletti, C. Ronco, M. Trovaslet, Y. Nicolet, L. Jean, P.-Y. Renard, Crystal structures of human cholinesterases in complex with huprine W and tacrine: elements of specificity for anti-Alzheimer's drugs targeting acetyl- and butyryl-cholinesterase, Biochem. J. 453 (2013) 393–399, https://doi.org/10.1042/bj20130013, 10.1042/BJ20130013.
[52] Molecular Operating Environment (MO, E), Chemical Computing Group ULC, Montreal, QC, Canada, 2014, 2014.0901.